AD-A124 672 A TIME INTEGRATING OPTICAL CORRELATOR FOR ADAPTIVE ARRAY PROCESSING(U) AIR FORCE INST OF TECH WRIGHT-PATTERSON AFB OH SCHOOL OF ENGINEERING 1/1

UNCLASSIFIED L B MERCER DEC 82 AFIT/GEO/EE/82D-5 F/G 20/6 NL

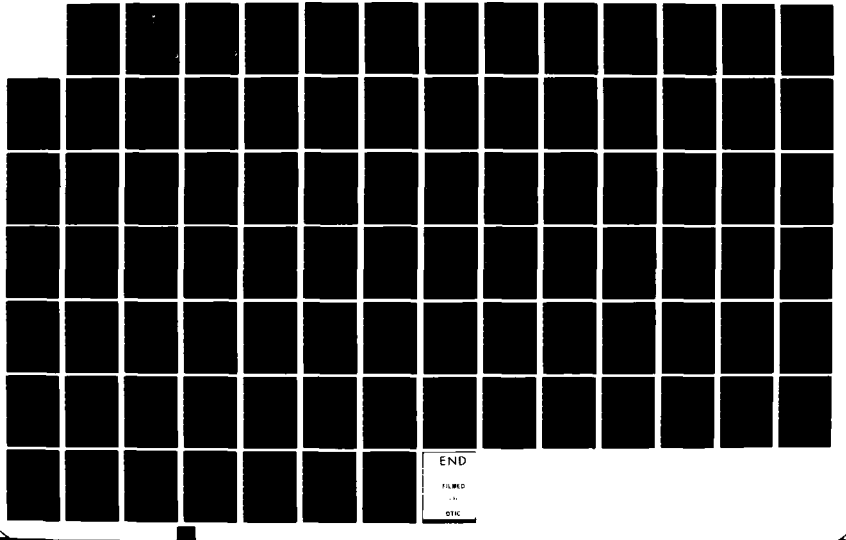

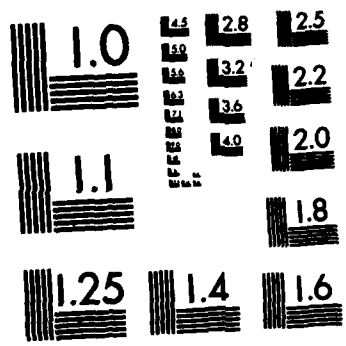

A TIME INTEGRATING OPTICAL CORRELATOR FOR ADAPTIVE ARRAY PROCESSING

Linden B. Mercer
Lieutenant USAF

AFIT/GEO/EE/82D-5

DEPARTMENT OF THE AIR FORCE
AIR UNIVERSITY (ATC)
AIR FORCE INSTITUTE OF TECHNOLOGY

Wright-Patterson Air Force Base, Ohio

AFIT/GEO/EE/82D-5

A TIME INTEGRATING OPTICAL CORRELATOR FOR ADAPTIVE ARRAY PROCESSING

AFIT/GEO/EE/82D-5

Linden B. Mercer
Lieutenant USAF

AFIT/GEO/EE/82D-5

A TIME INTEGRATING OPTICAL CORRELATOR FOR ADAPTIVE ARRAY PROCESSING

THESIS

Presented to the Faculty of the School of Engineering
of the Air Force Institute of Technology
Air University
in Partial Fulfillment of the
Requirements for the Degree of
Master of Science

by

Linden B. Mercer, B.S.
Lieutenant USAF

December 1982

Acknowledgements

This thesis began with the objective being determination of the performance of optical signal processing for adaptive arrays. The magnitude of the scope of this objective seemed at some points to grow faster than my understanding. God's understanding is unbounded and I thank Him for the assurance He gave me. I also thank my advisor, Lt Col Carpinella, for his guidance, patience, and assistance. My committee members, Maj Castor and Dr. Kabrisky, also deserve thanks for their assistance in reviewing my work. Finally, I would like to note my sincere appreciation for the encouragement and prayers of my family and friends.

Linden Beattie Mercer

Table of Contents

List of Figures

List of Tables

Abbreviations

AA - adaptive array

AO - acousto-optic

OSP - optical signal processing

TIOC - time integrating optical correlator

Abstract

Application of optical signal processing techniques to adaptive array processing was investigated. The common adaptive array algorithms were reviewed. Adaptive array processing generally requires some form of correlation and the characteristics of optical correlators were compared leading to the selection of the time integrating optical correlator for further investigation. An adaptive array processor using time integrating optical correlators, which was first proposed by David Casasent, was analyzed to determine applicability of this signal processing technique to a general adaptive array environment. This processor was found to be similar to a comparable maximum likelihood approach. Limitations on the performance of this processor in terms of ambiguity and resolution were found and these results were confirmed by computer simulation of the adaptive array environment, the processor, and the resulting antenna response.

I. Introduction

An adaptive array rejects interference by adjusting the amplitude and phase response at each of its elements to place nulls in the antenna pattern in the directions of the interference. Adaptive processing becomes complex as the number of adaptive weights increases. The use of optical signal processing offers numerous advantages over digital or electronic analog processors such as speed and parallel processing.

This thesis presents the results of an investigation of the application of optical signal processing to adaptive arrays. This investigation began with very few constraints on the directions to be pursued so a considerable effort was necessary to determine which areas of the problem deserved the most attention. The nature of the adaptive array problem was reviewed to provide an understanding of its signal processing needs. Optical signal processing was then surveyed to determine the possibilities of meeting these processing needs. Chapter II of this thesis reviews the adaptive array background and discusses some of the algorithms which have been developed for adaptive processing. A common factor in many of the adaptive algorithms is correlation and Chapter III provides an overview of the diverse possibilities for optical correlators. The time integrating form of optical correlator was chosen as the best for the adaptive array problem and Chapter IV presents the characteristics of

each part of this correlator with emphasis on the performance limiting aspects of each. An adaptive array processor utilizing time integrating optical correlation which was first presented by Casasent (Ref 1,2) and variations on this processor are the subjects of Chapter V. The concepts upon which this processor is based is to use a correlation of the signal present at the elements of the adaptive array to estimate the directions of the interference sources. This process is comparable to a maximum likelihood estimate of these directions. These directions must be used to determine element weights to null these direction. An efficient approach to this post processing task is presented which has considerable flexibility in terms of implementation. As part of this thesis the time integrating optical correlator and associated post processing were simulated. Details of this simulation are included in Chapter VI and the Appendix, and the results of this simulation and conclusions concerning optical signal processing for adaptive arrays and the performance of this particular time integrating processor are contained in Chapter VI.

II. The Adaptive Array

Introduction

An adaptive array (AA) rejects interference by placing nulls in the receiving antenna pattern in the directions of interfering signals. Ideally, this is accomplished without losing sensitivity in the direction of the desired signal. The adaptive array compensates automatically for spatial, temporal, and spectral variations in the signal plus noise environment. (Ref 3,2). Optimum matching of the temporal response of the system to the signal and noise waveforms contributes to the depth of the spatial pattern nulls (Ref 3.3). The temporal aspect of the system involves processing the incoming signals and continually adjusting the pattern to the changing environment. The active part of the adaptive array is the processor which uses some a priori information about the signal or noise and the signal plus noise inputs from the array to determine the amplitude and phase weighting of each element of the array which is optimum according to some given criterion. The criterion chosen and the constraints which are placed on the optimization lead to different forms of the adaptive array processor.

This chapter will first present some background including the notation, assumptions, and basic characteristics upon which later discussions of the adaptive array will be based. The remainder of the chapter will present an overview of the common

algorithms used for AA processing and the variations for different a priori knowledge as well as discussing important performance measures.

General Structure

The general form of the adaptive array as shown in Fig. 1 consists of the antenna array, fixed processing, element weights, and the weight controlling system or AA processor. A given system may combine these in different ways and different processors may use some subset of the inputs shown. The notation which will be used in this thesis for AA discussions is given in Table 1.

Array Configuration

The antenna elements may be arranged linearly, circularly, or even randomly. The performance of the array can be limited or enhanced by different geometries (Ref 3:23) and the form of the processor is different for different geometries. A linear array of evenly spaced elements was chosen for this thesis. This choice leads to a simpler processor for the processing approach investigated. Variations in element spacing for the linear array result in varying null widths and thus are important to AA performance. (Ref 3:20). However, the form of the processor is not affected so no further assumptions will be made on this point.

Antenna Response

The linear array with the equally spaced elements exhibits an equal dealy from element to element for a signal for a directional

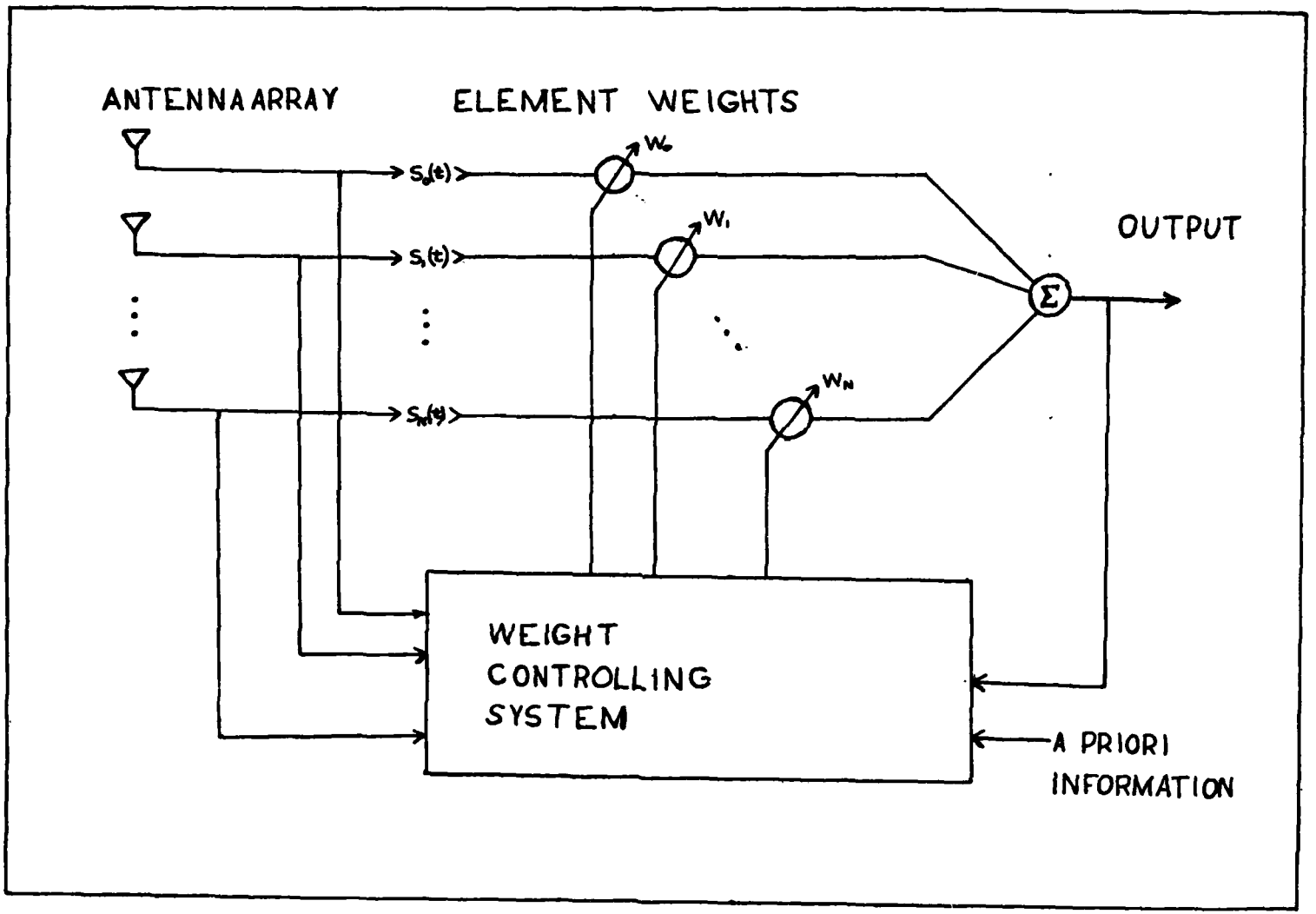

Fig. 1. Adaptive Array Processing Structure

source which is sufficiently distant to be represented as plane wavefronts. The delay for a source at an angle θ off of boresight is given by

$$\tau = \frac{d}{c} \sin\theta \qquad (1)$$

where d is the element to element spacing and c is the speed of signal propagation. This equation is easily seen from Fig. 2.

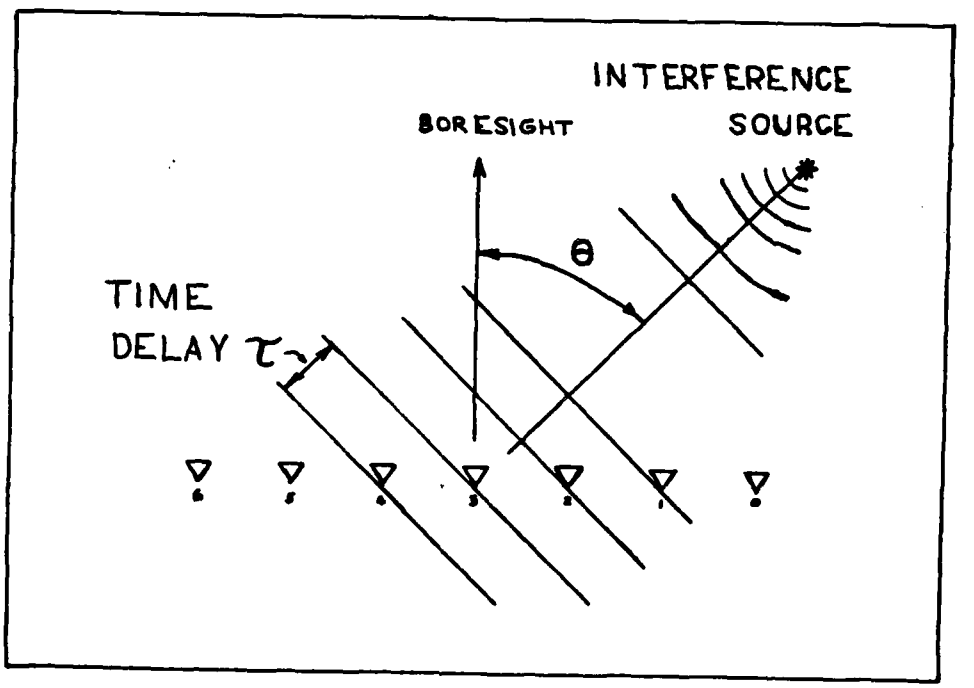

Fig 2. Element-to-Element Time Delay

Table 1. Adaptive Array Notation

N	-	Number of elements - 1
n	-	A given array element (element zero is far right)
K		Number of directional noise sources
k	-	A given noise source
d	-	Center to center separation of elements
λ	-	Wavelength of radiation
$r_n(t)$	-	Signal received at element n
θ_k	-	Angle of source k from bore sight.
θ_d	-	Angle of source off of bore sight
τ_k	-	Delay of source k from element to element
$\underline{W}$	-	A vector of the complex weights applied to each element
W_n	-	The weight applied to the nth element
$S_k(t)$	-	Signal process from noise source k as received at element zero
$S_d(t)$	-	Desired signal as received at element zero
$\underline{M}$	-	Signal-plus noise covariance matrix

For a source with frequency, f, the phase delay is thus

$$\phi = 2\pi f \frac{d}{c} \sin\theta \tag{2}$$

The AA multiplies the signal at element n by some weight, W_n, so the far field response of the array can be found to be

$$B(\theta) = \sum_{n=0}^{N} W_n \exp(jn2\pi f \sin\theta) \tag{3}$$

where far field can be taken mean distances so much greater than the largest dimension of the array.

Input and the Covariance Matrix

The general form of the input and the covariance matrix are presented here for later reference. The input signal $r_n(t)$ at element n can be written in the following form:

$$r_n(t) = S_d(t-n\tau_d) + \sum_{k=1}^{K} S_k(t-n\tau_k) \tag{4}$$

for a desired signal at some angle θ_d from bore sight and K directional noise sources at angles θ_k. Note that $S_d(t)$ and $S_k(t)$ are the signals as received at element zero, the far right element looking towards bore sight and that they may be deterministic or random in nature. The delay of each signal at element n is thus $n\tau$ where τ is as defined in eq. (1).

The covariance matrix, $\underline{M}$, is made up of the covariance terms

$$M_{ij} = E(r_i\ r_j) \tag{5}$$

The resulting matrix is fundamental to AA theory. The terms are determined by the power and spatial distribution of the noise sources. The desired weight vector, $\underline{W}$, can be shown to be the result of a vector matrix product,

$$\underline{W} = \underline{M}^{-1}\ \underline{S} \tag{6}$$

where $\underline{S}$ is a steering vector which determines the direction of the main beam (Ref 4:586 and 1:6).

Algorithms

This section will briefly review the common algorithms which have been developed for AA processing. Most of the algorithms which have been developed to find the weight vector, $\underline{W}$, for a given noise environment can be derived as an optimal solution based on a particular performance criterion. These algorithms and their associated performance criteria are:

LMS - Minimizes the mean square error between the array output signal and a reference signal

MSN - Maximizes the output signal to noise ratio

M L - Finds a maximum liklihood estimate of the signal information

MNV - Minimizes the output noise variance

Other algorithms which have been developed include the SMI or sample matrix inversion approach and the RS or random search method.

LMS. The LMS algorithm was developed by B. Widrow (Ref 5) and it has probably received the most widespread application (Ref 3:9). There are several variations, but in general, a reference signal is subtracted from the output and the result is correlated with the incoming signal at each element. Many references are available detailing the theory and performance of this algorithm (Ref 5,6,7).

MSN. The maximum signal to noise ratio (MSN) algorithm was developed by P.W. Howells and S.P. Applebaum (Ref 8). This algorithm is the result of radar side lobe cancelling work. A generalized output signal to noise ratio is maximized by means of a steering signal at the element weights. Both the MSN and LMS algorithms derive their weight control from a correlation between the signals at each of the elements and both converge toward the same solution (Ref 4).

ML. The maximum likelihood (ML) algorithm produces an estimate of the desired signal which is the most likely waveform. This optimization requires known second order statistics of the noise and generally assumes a Gaussian distribution (Ref 6:3-4, 3-10). This algorithm requires no knowledge of the signal except that it is deterministic.

MNV. The minimum noise variance (MNV) algorithm minimizes the output noise variance (Ref 6:3-2). This algorithm assumes known

direction of arrival and zero mean noise sources such that the output after correction for the direction of arrival is an unbiased estimate of the desired signal. This method also requires no knowledge of the signal and only second order statistics of the noise.

SMI. The sample matrix inversion (SMI) algorithm is an example of a higher order processing algorithm. A direct calculation of the optimum weights is made based on sampling the signal at each element and inverting the resulting noise covariance matrix (Ref 3:11). This method produces the weights directly but is computationaly complex.

RS. The random search (RS) algorithm varies the weights in a random or nearly random manner in such a way as to continually improve some performance measure (Ref 3:11 and Ref 6:4-2). This is basically a refined trial and error approach. This has the advantage of simplicity, however, some guidance must be added to this search and in general, the search techniques do not lead to practical circuitry (Ref 6:4-5).

Optimization Techniques (Ref 6). The technique employed by each algorithm to optimize the array weights directly affects the rate of convergence. These algorithms can basically be categorized as search (zero order), gradient (first order), or higher order techniques. Most algorithms which have been investigated including the LMS, MSN, ML, and MNV use the first derivative of the performance criterion and converge on the optimum point by adjusting the weights to move in the direction of steepest descent towards the optimum

weights. The rate of convergence is determined by the size of the adjustment made at each step. The size of this adjustment is the gain of the feedback loop and as with any control loop the choice of this parameter is critical to the speed or adaptation time and the stability of the processor. Higher order methods effectively use some information about the second or higher derivatives and thus, these methods are able to produce a set of weights which are optimum by performing only one iteration. The trade-off which must be considered is between complexity of a higher order systems and slow convergence of lower order systems.

Summary of Algorithms. The algorithms discussed provide a general overview of the types of AA processors. There are untold variations on these approaches and others which were not discussed. Although the criteria which these algorithms optimize are different, they all approach the same results. One of the major differences is difficulty of implementation and another is the rate of convergence to the optimum set of weights. Convergence has been discussed here and the reader is referred to Ref. 6, Chapter X for a discussion of implementation.

A Priori Knowledge

The form of the AA processor is dependent upon the information which is known a priori. The AA basically eliminates unwanted signals by adding two or more signals which have phase differences such that their sum is zero. To discriminate between signal and noise some a priori knowledge must be available (Ref. 3:13). This

information might be the waveform, spectral information, directions of arrival (DOA) , polarizations, or power levels. The knowledge might be about the noise or the signal and of course, many combinations are possible.

Performance Measures (Ref. 3:17-19)

Adaptive arrays differ greatly from one algorithm, or implementation or set of a priori information to another. As a result, the performance measures used to characterize them are diverse and comparison can be difficult. Each adaptive array emphasizes certain criteria which are important to a particular application. Some of these characteristics include the bandwidth over which the nulls exist, the number of array elements, signal optimization, or all signal suppression, adaptation time, and number of sources to be nulled. Operating characteristics such as the ability to retain nulls for intermittant jammers, called null memory and the methods used to acquire the desired signal are also important.

A common point for comparison is null depth. This measure is analogous to processing gain in a spread spectrum system. Direct comparison, however, of this measure may be inappropriate due to differences in bandwidth or adaptation time. A useful measure of an adaptive array is the improvement of signal to noise ratio at the output since more factors are included in its determination. In general, the specific needs of the application and a number of the performance measures which have been mentioned must be taken into consideration for any valid comparison.

Summary

This chapter has presented some background information concerning adaptive arrays. The general form of the array and its processor were presented and some related notation and the response at the array output and input were introduced. A number of processing algorithms were briefly discussed and some related topics were included. Finally, an overview was made of some of the performance measures used for adaptive arrays. This background will be the basis upon which presentation of the time integrating optical correlator for adaptive processing will be made.

III. Optical Signal Processing

Introduction

Optical signal processing (OSP) is one of the answers to the technological problem of processing large quantities of signal information for real time applications. Optical signal processing architectures and algorithms begin with electrical signals, convert the electrical signals to light signals, process the light, and convert it back to the electrical signal which is the desired product. This chapter will present some of the background needed for a good understanding of OSP and then some of the architectures which have been developed will be briefly presented. The emphasis here will be entirely on correlating processors since correlation is a common factor in most of the adaptive array algorithms.

Background

Light Propagation. This section will briefly discuss some of the light properties which are used in OSP. The propagation of light as a wave can be represented by the Huygen-Fresnel equation. This equation can be simplified in the far field or in the focal plane of a lens and the result is the Fraunhoffer equation. In the focal plane of a lens the Fraunhoffer equation reduces to a constant times the two dimensional Fourier transform of the amplitude distribution of the light entering the lens. This is, perhaps, the most important optical

property used in OSP. Using this property a transformation can be made from the time domain to the frequency domain at the speed of light with only a simple lens system. This same property, however, also limits the ultimate resolution obtainable with any common optical system. The smallest resoluable area is limited by diffraction through the optical system. The resolution limit for an aperture whose size is given by d in a particular direction is about

$$\delta = \frac{\lambda d}{L} \tag{7}$$

in that same direction where λ is the wavelength of light being used and L is the distance from the aperture. The properties discussed to this point can all be obtained through Fourier optics (Ref 9).

Modulators

All OSP systems can be broken down into three parts; the light source, a light modulator or modulators, and the detectors and the optics. These will all be discussed more later but some of the common light modulators will be presented here in order that later discussions may be limited to only one type. Some of the devices which have been used are listed here:

1. Acousto-optic cells
2. Liquid crystal light value (Ref. 10).
3. Thermo plastic optical phase devices (Ref. 10)
4. Electro-optic cells

Only the first three have the ability to spatially modulate light and only the acousto-optic (AO) cell has the speed which is needed

for signal processing applications. Although technological improvement may make other systems viable in the future, only acousto-optic systems will be investigated in this thesis.

Correlator Characteristics. The following sections will present some of the OSP architectures which have been proposed to perform the operation of correlating two signals. The correlation to be performed is given here

$$S(t) = \int_0^T S_1(t')\, S_2(t+t')\, dt' \tag{8}$$

Commonly, one of these signals is a reference signal and the other is a received signal containing both signal and noise. Some basic characteristics of this correlation are important in understanding a comparison of the processors to be discussed. The first is the width of the correlation peak output.

The correlation of a simple pulse of length T_s, with a similar pulse produces a correlation of width 2T. This signal has a $sinc^2$ frequency distribution with a main lobe width of $2/T_s$ as shown in Fig. 3. The width of the correlation peak is the reciprocal of the main lobe bandwidth yielding an approximation for the relationship between bandwidth and correlation width of

$$W \triangleq \frac{1}{B} \tag{9}$$

where B is the bandwidth of the signals being correlated (Ref 11:136).

Another important characteristic is the power signal-to-noise ratio of the correlation output as compared to the signal-to-noise of the noisy signal $S_1(t)$

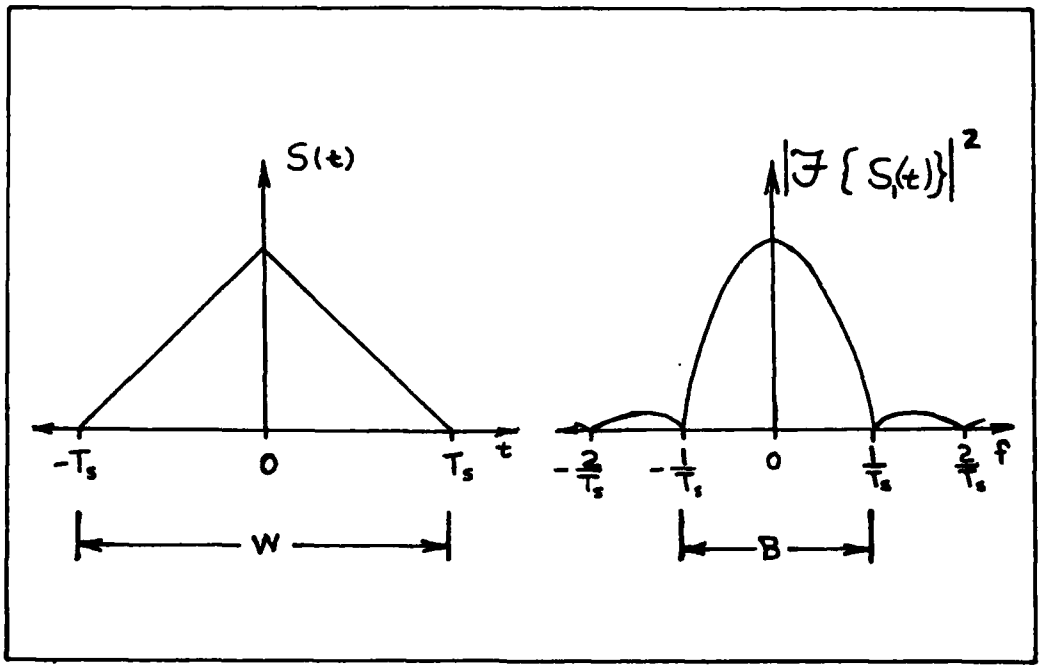

Fig. 3. Correlation Width and Bandwidth

$$SNR \triangleq BT\ SNR_1 \tag{10}$$

where SNR_1 is the signal-to-noise of $S_1(t)$, T is the correlation time, and BT is the time bandwidth product of the correlator (Ref. 11:137). The gain is reduced if the bandwidth of the signal is less than the bandwidth of the correlator or if the duration of the signal is shorter than the integration time. The correlator thus exhibits a gain in signal-to-noise called correlation gain or processing gain, equal to the time bandwidth product of the processor. The correlation time, T, is called the time window. Another parameter called the range window is the time error allowed between the received and reference signal. The received signal may in fact be composed of the reference signal delayed by some quantity, τ, plus the noise signal

$$S_1(t) = S_2(t-\tau) + n(t) \tag{11}$$

If this error, τ, is greater than the time window, T, no overlap of the signals will occur where the reference portion of the received signal and the reference signal coincide.

These four parameters

1. Bandwidth
2. Time with product
3. Time window
4. Range window

can be used to compare the OSP configurations which are available for AA processing.

OSP Architectures

Spatial Integrating. The simplest and the tranditional form of acousto-optic correlator performs the integration operation over a spatial coordinate. This correlator first produces a light wave whose amplitude, phase or intensity is a spatial representation of one of the signals to be correlated. This light wave is then further modulated by the second signal which produces the product along a spatial coordinate. Integration along this coordinate is performed by focusing this product onto a point detector. The spatial light signals can be produced by AO modulators and as the signals propagate through the modulators, the signal from the detector is the correlation for different time delays. A schematic of this type of correlator is shown in Fig. 4. Notice that the signal into the second cell must be the reference signal time reversed in order for the correlation to be formed. The two AO cells can in fact be combined into one cell to produce a very compact unit which requires very few optical

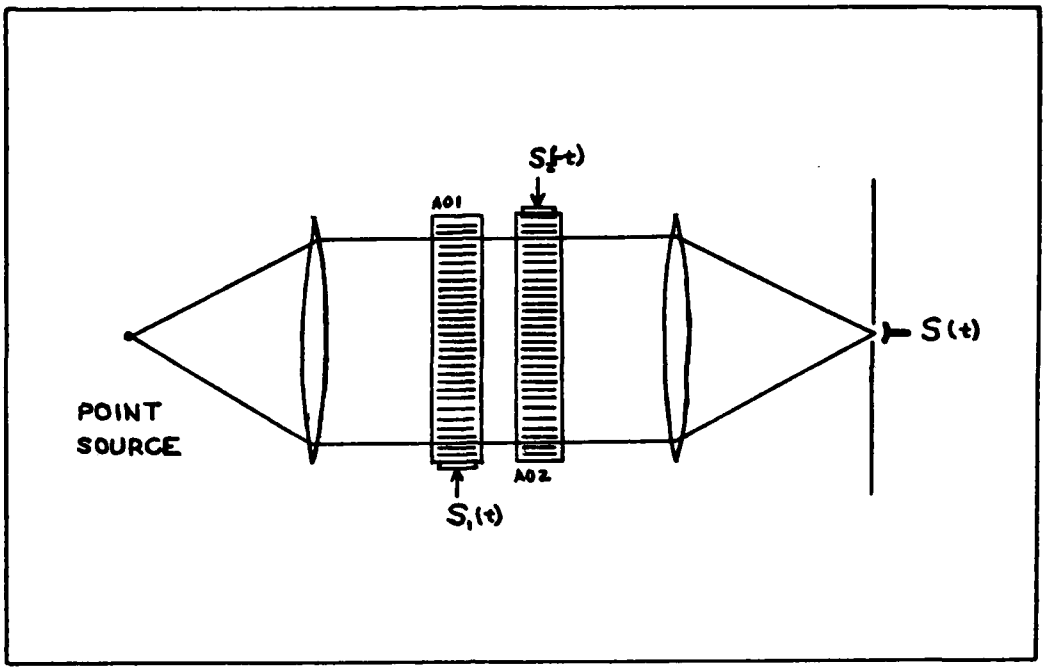

Fig 4. Spatial Integrating Correlator

elements and is easily aligned (Ref. 11:140). Many variations on this general idea are in fact possible. For a known reference signal a fixed mask may replace one of the AO cells. It should be pointed out that the figure shown is only a schematic. Variations which may be made, involve such things as using coherent or incoherent light. With coherent light, a complex correlation may be performed using heterodyne detection (Ref. 12:70). For this type of detection, the modulators actually phase modulate the light wave and this phase modulation is converted to amplitude modulation (Ref. 12:67). Other spatial integrating architectures use the Fourier transform property of light diffraction. A unique form of the spatial correlator called a chirp correlator detects the time of arrival of linear

frequency modulated pulses (chirps). The acoustic wave modulated by the chirp acts as a Fresnel zone plate which focuses light on a detector providing the desired correlation (Ref. 11:14).

The system specifications for these different forms of spatial correlators are largely determined by the AO cell. The maximum signal bandwidth is the bandwidth over which the AO cell operates efficiently and with acceptable distortion. Detectors are available which do not limit this bandwidth. The time window is limited to the time window of the AO cell since integration is performed spatially along the length of the cell. The time bandwidth product or gain of the correlator is the product of these and thus is determined solely by the AO cell. AO cells can be produced with time bandwidth specifications as high as 1600 (Ref. 13:2). The range window of the correlator as shown in Fig. 4 is limited to the time window of the AO cell. This is because even for very short pulses the signals must be present in both cells to produce a correlation. The second cell may be replaced by a reference mask for a known signal and the resulting range window is infinite. The range window for the chirp correlator is also infinite since no reference is used.

Time Integrating. The basic form of the time integrating acousto-optic correlator is shown in Fig. 5. The intensity of the light source is modulated by $S_1(t)$ and the product, $S_1(t)\ S_2(t+t')$ is formed in the AO cell. The time delay t' is determined by the position in the cell and velocity of propagation of the acoustic wave. The product is then integrated in time at the detector array which is in general a CCD array.

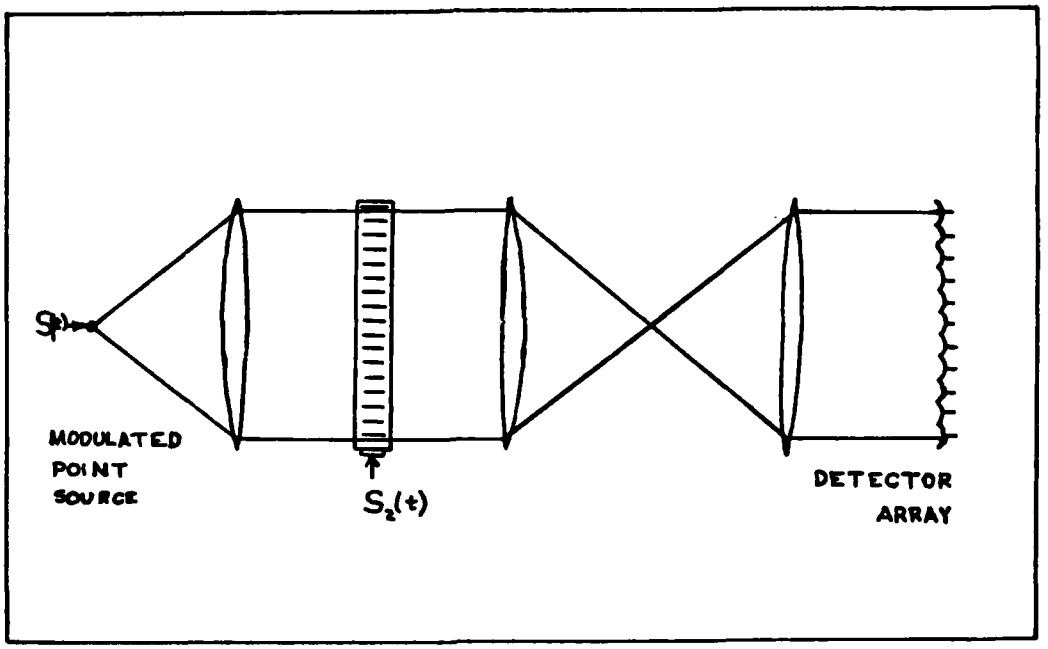

Fig. 5. Time Integrating Correlator

To better understand the processes taking place in the time integrating processor, it is helpful to trace the signal progression through the system as shown in Fig. 6. The system being described uses a modulated point source collimated by a cylindrical lens. Shown in part 'a' of that figure are the light pulses traveling towards the AO cell and another pulse which is the input to the AO cell. In 'b' the light pulses have just entered the cell. In 'b' and 'c', the light pulse which is the result of the second signal is shown exiting the cell along with the first pulse. The second signal is drawn slightly taller for identification and the product formed is shown in part 'c' by the cross hatched area. The detectors integrate the product over time and output the result at the end of the integration time. Shown in part 'd' at the detectors is the output for the case shown. Due to the delay as the pulse travels through the AO cell the pulses are synchronized in time only along one ray of light, thus

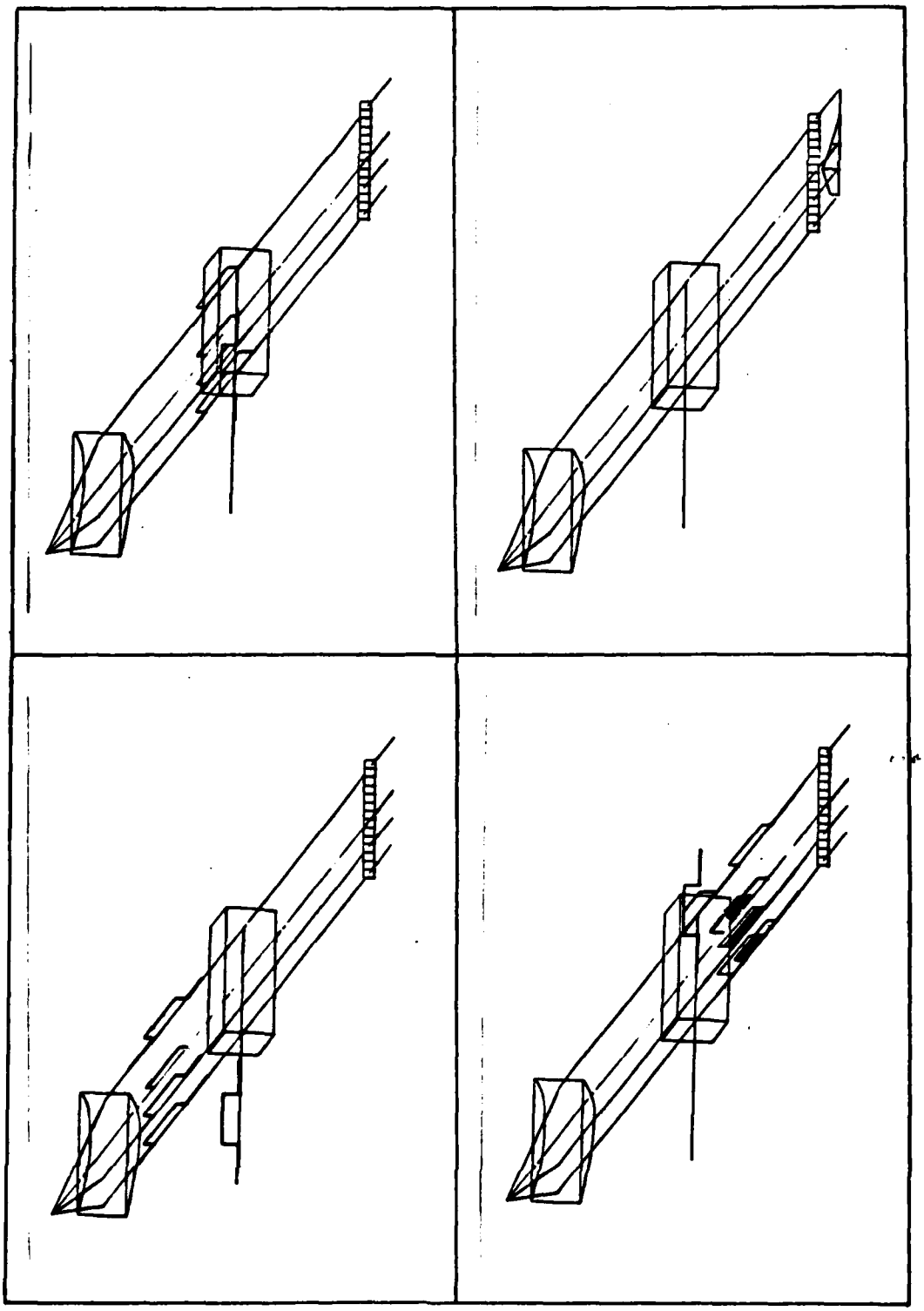

Fig. 6. Time Integrating Correlator Operation

producing the peak output at this point.

Another time integrating optical correlator (TIOC) schematic is shown in Fig. 7. This architecture uses two AO cells (or one cell with two acoustic channels). The product is formed as the light is modulated by each of the cells and the result is integrated in time by the detector array.

The maximum signal bandwidth for the TIOC is also limited to the bandwidth of the AO cell. The time window of this processor is the time over which the detector is allowed to integrate. This time window is thus infinite, however, the time bandwidth product or gain in signal to noise ratio is limited by detector noise. The maximum signal to noise voltage ratio for the CCD array is given by its dynamic range, D. The time bandwidth product is effectively D^2 (Ref. 11:143). In fact, there are other noise and bias sources which reduce the gain but detectors are available with dynamic ranges of 10^3 (10^4 with cooling) so very high gains are possible. The range window of the TIOC is limited to the time window of the AO cell.

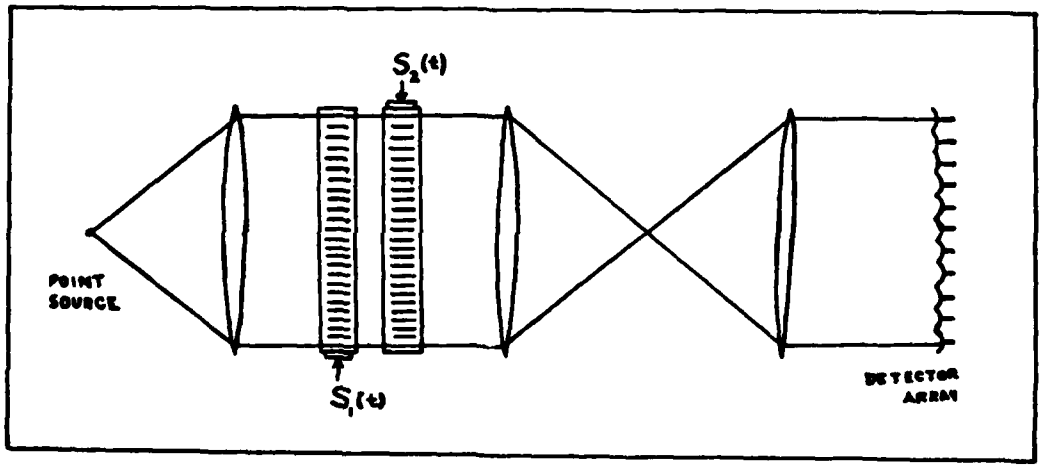

Fig. 7. Two Cell Time Integrating Correlator

Comparison and Conclusions

To determine the ability of these correlators to provide AA processing needs, a comparison of their basic correlation parameters can be made. A summary of correlator specifications is given here in Table 2 as taken from (Ref. 11).

Table 2. Correlator Comparison

	Bandwidth	Time Window	Time Bandwidth Product	Range Window
1. Spatial integrating				
a. Fixed reference mask	B	τ	$B\tau$	∞
b. Two cell correlator	B	τ*	$B\tau$*	τ
c. Chirp correlator	B	τ	$B\tau$	∞
2. Time integrating	B	∞	D^2	τ

B = bandwidth of AO cell
τ = time window of AO cell
D = detector dynamic range

*Assuming complete overlap of the two signals for short pulses

The space integrating and time integrating systems each have advantages and disadvantages. The space integrating system has a limited time bandwidth capability but is capable of searching over a large range window or delay in time of arrival. The time integrating system allows processing of large time bandwidth product signals thus producing significant gain; however, the range window is limited (Ref. 14:42). For the AA processing needs, the signal delay is never longer than the propagation delay between the most widely separated elements. Time

windows for AO cells are commonly several microseconds so the range window is not an important consideration for AA processing. The time integrating optical correlator shows the greatest potential for AA processing particularly for signal environment, with large time bandwidth signals. The time integrating systems achieve processing gain over the full duration of a signal (up to the limits set by dynamic range) whereas the space integrating system is limited to durations of several microseconds. Because of these observations, further investigation of OSP in this thesis is limited to acousto-optic time integrating correlators.

IV. Time Integrating Optical Correlators

The basic form and the correlation specifications for the time integrating optical correlator (TIOC) were presented in the last chapter. This chapter investigates the characteristics of each part of the TIOC with particular emphasis to those aspects such as noise which limit the overall performance.

The parts of the TIOC which will be examined are the source, the AO modulator, and the detector. Other parts of the TIOC which will not be discussed are the optics and the electronics which drive the AO cell and process the detected signals. The lenses required for these systems may be obtained with sufficient quality that they do not, in general, limit the performance of the system. It should be noted, however, that very high quality optics must be specified for heterodyne detection where phase information must be maintained.

AO Modulators

Theory. This section will present some of the basic theory of acousto-optic cells necessary to understand the operating limitations and first order design criteria of these cells. Bragg diffraction can be thought of in somewhat the same way as X-ray diffraction in a crystal with the atomic planes replaced by the planes of compression and rarefaction introduced by ultrasonic sound waves (Ref. 15:4). The velocity of the sound waves causes the diffracted light to be Doppler shifted. As

shown in Fig. 8, a beam of light is directed into the path of the acoustic wave inside the cell. At certain angles of incidence $\pm \alpha_B$, a

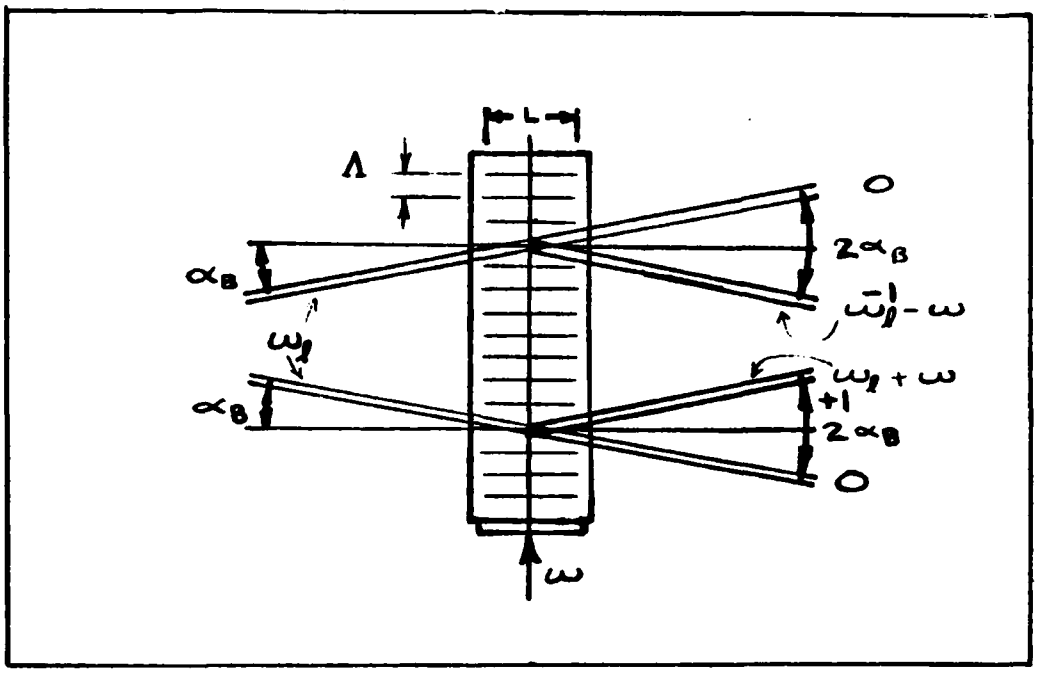

Fig. 8. Bragg Cell Diffraction

diffracted beam is produced whose direction differs by $2\alpha_B$. The angle α_B is called the Bragg angle and is given by

$$\sin \alpha_B = \frac{\lambda}{2\Lambda} \tag{12}$$

where λ is the optical wavelength and Λ is the acoustic wavelength. This type of interaction results in only a single first order diffracted beam and the portion of the origianl beam which is not diffracted. In the figure shown, the effect of refraction according to Snell's law is omitted for simplicity.

The interaction between the light and acoustic waves may fall into one of several different regimes depending upon the optical and acoustic properties of the material used, the optical and acoustic frequencies used, and parameters of the cell and input transducer. In the Raman-Nath regime, also known as the Debye-Sears or Lucas-Bequard region, the light enters parallel to the acoustic wave fronts and many positive and negative orders of diffraction are produced. The Raman-Nath type of operations are limited to low frequencies and small bandwidth. (Ref. 16:131). Increased bandwidth and higher frequency operation requirements have led to widespread use of the Bragg regime. This type of operation which was shown in Fig. 8 is characterized by the requirement that light must enter at the Bragg angle and only a single diffracted beam is produced. Recently, a new group of materials for which other regimes of operation are possible have been investigated for use in OSP. Birefringent materials exhibit different indices of refraction for differently polarized beams of light and the properties differ according to different directions of propagation relative to the crystal structure. Birefringent crystals present greater versatility and improved characteristics for signal processing. The birefringent cells are capable of high frequencies and large bandwidths. Either a single first order or positive and negative first order outputs may be produced depending on the construction of the cell.

The essential properties of the interaction taking place in all acousto-optic cells may be explained by considering the interaction as a collision between photons and phonons (Ref. 21:49). Conservation of momentum is satisfied. The moments of the particles are given by $\hbar \underline{k}$ and $\hbar \underline{K}$ for the photons and phonons respectively, where $\hbar = h/2\pi$

and h is Planck's constant. The propagation vectors of light and sound $\underline{k}$ and $\underline{K}$, have magnitudes $2\pi/\lambda$ and $2\pi/\Lambda$, , respectively and their directions are the directions of propagation. From the wave vector diagrams in Fig. 9 for Bragg diffraction the Bragg angle is seen to be given by

$$\sin \alpha_B = \frac{1}{2} \frac{K}{k} = \frac{1}{2} \frac{\lambda}{\Lambda} \tag{13}$$

as given earlier in (12). Both down shifted and up shifted interactions are shown. These shifts can be found from the conservation of the photon and phonon energies $\hbar\omega$, and $\hbar\omega$ (Ref. 15:49). The angle at which deflection takes place is related to the frequency content of the acoustic wave by the magnitude of $\underline{K}$. The cell, therefore, naturally analyzes the spectrum of the signal input to the cell. Note that for the interaction to take place, $\underline{K}$, and thus the frequency input, must be within a limited range. The proportion of the input beam which is deflected is related to the power contained in the acoustic wave.

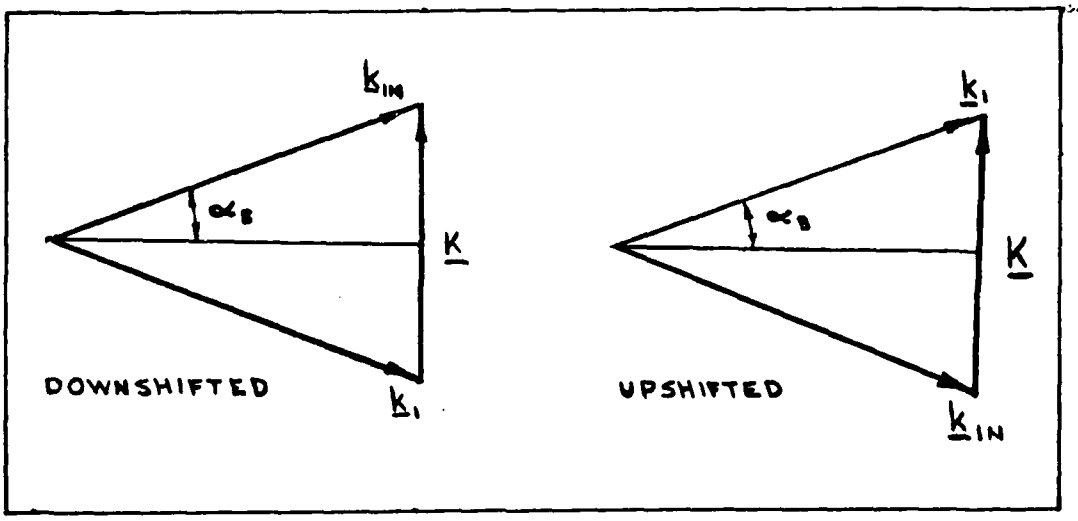

Fig. 9. Propagation Vector Diagrams

The relative light intensity of the first order diffracted light beam for Bragg diffraction has been given as (Ref. 17:54)

$$\frac{I_1}{I_o} = C\ P_A\ \text{sinc}^2 \left| C\ P_A + (\Delta k\ L/2)^2 \right|^{\frac{1}{2}} \qquad (14)$$

where I_1 and I_o are the intensities of the diffracted beam and the input beam, P_A is the acoustic power, Δk is the momentum mismatch of the light and acousto-optic propagation vectors, is the width of the acoustic beam and C is constant which depends on the proper ties of the cell material and its dimensions. Obviously, the response of the cell is not in general linear either for amplitude or intensity modulation.. To achieve linear operation, the cell is operated only over limited ranges and efforts to reduce the effects of the momentum match Δk.

The design parameters associated with AO cells are efficiency, bandwidth, resolution, distortion and dynamic range. The efficiency of the cell is measured by the percentage of the input beam which is deflected per watt of acoustic input. The input transducer is generally limited to less than one watt so a cell which has poor efficiency can limit the optical ouptut for a given input light source. AO cell efficiencies range from 1 to 300 %/W.(Ref 10:2). The bandwidth limitations of the cell are due to a number of sources including the input transducer, (Ref 16:183), the width of the optical beam and acoustic beam charactersitics resulting in momentum mismatch. AO cells have been fabricated with bandwidths of 40 to 1000 Mhz.(Ref 13:2). The techniques used to increase bandwidth are varied, however, in general bandwidth increases can only be obtained by sacrificing other performance

characteristics such as aperture and efficiency.

The resolution of the AO cell is important to the performance of the TIOC. This performance is affected by the information capacity of the cell which can be approximated by the length of the time window which is the aperture multiplied by the bandwidth of the cell. The resolution is further limited by diffraction. Elements which are resolvable at the AO cell any not be resolvable at the defector due to diffraction. The diffracted image has reduced resolution due to spreading of the beam and also the sidelobes produced. The effects of the sidelobes can be reduced by apodization of the optical beam (Ref. 16:136). The resolution of the cell is also improved by increasing the aperture and the bandwidth thereby increasing the time bandwidth product, however, as mentioned, increased bandwidth is usually accompanied by shortened apertures. For the purpose of this thesis it will be assumed, as is the common practice (Ref. 1:33), that the number of resolvable points in the image plane is equal to the timeband width product. AO cells have been produced with timeband width products of as high as 1100 for a bandwidth of 1.05 GHz or 1600 for 40 MHz bandwidth.

A number of nonlinear characteristics are present in the AO cell which can contribute to distortion both in the amplitude or intensity of the modulated output and in its phase. The sources of the limitations and the techniques used to counteract them are too numerous and complex to be included in this thesis.

The dynamic range of the AO cell is limited by the range of the acoustic input transducer, and by the regions of operation over which the overall response is linear. This parameter is important because of the restriction it imposes on the signals which can be

processed using these devices. Cells have been produced for which dynamic ranges have been claimed to be as high as 80 dB; however, 60-65 dB is a more realistic limit for today's technology (Ref. 10:2).

Sources and Detectors

Sources and detectors for TIOC will be discussed here together since the random fluctuations in the light sources will most easily be described in terms of the noise which results upon detection. The sources which will be discussed are the laser, laser diodes (LD), and light emitting diodes (LED). The detectors required for the TIOC are produced as arrays of photo diodes whose outputs are integrated and then read out at the end of the detection period.

Sources. The nature of the "noise" present in light from different sources can be described by the variance of the photo electron count during the observation time T_o. This noise is commonly referred to as shot noise. For an ideal monochromatic (zero line width) source the counting statistics are independent over disjoint observation periods resulting in a counting process which is Poisson. The variance of the count Q is

$$\sigma_Q^2 = E\{Q\} \tag{15}$$

where E{Q} is the expected value of the count over the observation period. If a laser is designed carefully to produce only a single temporal mode the line width may be made very narrow, therefore,

is a good estimate of noise variance exhibited. Most lasers, however, are designed to produce several temporal modes to increase output power. These modes are at different wavelengths and their random phase variations introduce beat noise also referred to as excess photon noise (Ref. 18:696,19:732, and 20:16). This produces a Bose-Einstein counting distribution similar to that for thermal photon generations where the variance is

$$\sigma_Q^2 = E\{Q\} + E^2\{Q\} \qquad (16)$$

This expression is valid where the coherence time remains much greater than the observation time and the coherence area is much greater than the detector area. The excess noise term can be very large for large counts. This situation should obviously be avoided for communications or optical signal processing applications.

It is noted by Pratt (Ref. 20:16) that phase locking the modes of the laser eliminates the random nature of the mode beating returning the laser to Poisson statistics.

The laser diode (LD) is typically less coherent than other forms of the laser resulting from the large number of laser lines or temporal modes which are exited. The bandwidth of the laser diode output may be on the order of 500 Ghz containing perhaps twenty laser lines (Ref. 21:96). The light emitting diode (LED) emits over a bandwidth on the order of 20-30 THz. The noise variance for these sources is given by

$$\sigma_Q^2 = E\{Q\} + E^2\{Q\} \frac{T_c}{T_o} \frac{A_c}{A} \quad T_o >> T_c, \quad A >> A_c \tag{17}$$

where A_c is the coherence area, A is the detector area, T_e is the coherence time, and T_o is the observation period. The coherence time for a multimode LD is about 29 pico seconds or less (Ref 21:98) and the coherence time for the LED is on the order of pico seconds which is about the same as from a thermal source. For reasonable observation times, the ratio T_c/T_o is very small and the ratio A/A_c which represents the number of spatial modes received is very large. For the LED the excess photon noise is certainly negligible and depending on its coherence this term may also be neglected for the LD source.

An important point to note here is that in general incoherent systems using LED sources use intensity modulation of the light output. Light detectors respond to incident power so this method produces linear output response to the input signal. Coherent systems on the other hand may use amplitude modulation of the light field thus requiring heterodyne detection at the output. Even in coherent systems using direct detection difficulties may be encountered due to phase errors introduced by the optics or the modulation process resulting in interference problems and degradation of system performance.

Detectors. (Ref. 22). The detectors required for the TIOC must be able to resolve at least as many points as the number of resolvable points in the AO cell and they must provide an integrated output. These requirements are generally approached using CCD or CID photo detector arrays (charge coupled devices or charge inspection devices). This section will present a brief discussion of each of the noise sources

present in these devices and discuss some other specifications pertinent to the TIOC performance.

The temporal noise sources in the detector array include thermal noise (Johnson noise) associated with charging capacitors through a resistance, shot noise due to leakage current, the shot noise of bulk traps in MOS-CCDs and the photon noise which was discussed in association with light sources (Ref. 22:108). The detector arrays perform integration by first charging a capacitor associated with each array element to a known value. The detected photo-electrons discharge the capacitor and the integrated signal is determined by the difference between the original charge and the charge remaining after detection. Both charging and discharging (read out) of the capacitor introduce noise. The variance of this noise is directly related to the temperature of operation so cooling is sometimes used to improve performance. The leakage current or dark current introduces shot noise with Poisson statistics. This adds to the variance of the output and is also detrimental because it discharges the preset charge in the readout capacitance, thus, limiting the dynamic range of the device. Another noise source is bulk trapping noise. The contribution from this source is very small except for cooled arrays with long integration times (Ref 22:109) and its details will not be discussed here except to note that it presents a nonPoisson shot noise.

An important source of noise for all detector arrays is fixed pattern or spatial noise due to nonuniform response across the array. This noise is due to a large number of sources within the detector. Post processing can be used to compensate for this noise but this approach is not practical for the number of elements needed for TIOC.

The effects of all of these noise sources is to reduce the dynamic range of the device. Dynamic range is defined here to be the ratio of the maximum photo electron count detectable which is limited by the initial charge placed on the capacitor and the minimum detectable photon count which is limited by the initial charge placed on the capacitor and the minimum detectable photon count which is limited by the noise count due to all of the noise sources discussed. Dynamics ranges of 10^3 to 10^4 (cooled) are possible with current technology. It was noted in Chapter II that this dynamic range limits the gain of the TIOC. This limit can be overcome, however, by multiple readout during the integration as well as other methods (Ref 22:108).

Summary

This chapter has presented some of the operating characteristics of AO modulators, light sources and detector arrays as they are used in time integrating optical correlators. The limitations of these devices have been presented and for many of the important paraments current device capabilities have been cited. The numerous variations on the architecture of this processor which are possible have not been discussed. However, it is important to note that time integrating correlators may be constructed to produce either real or complex correlations. For complex correlations, the processor must either perform four real correlations using quadrature components of the complex signals or the processor must be capable of detecting both phase and amplitude of the correlation product by using some form of heterodyne or interferometric detection. The interferometric detection can be performed by using co-

herent light and a local oscillator or it might also be accomplished in an incoherent system as described by Kellman (Ref 23). Another aspect of this processor which has not been discussed is the bias levels required both at the source and in the A0 cell to represent both positive and negative quantities. These bias levels are different for each architecture and thus cannot be specified in general, however, their effect on system performance is to reduce the dynamic range of the correlator output thus limiting the overall processor gain.

This thesis, having noted the limitations of the components of the time integrating optical correlator will assume that the correlator response is linear while keeping in mind the resolution and dynamic range limitations for which this is true.

V. A Time Integrating Optical Correlator Adaptive Array Processor

Introduction

The previous chapters have presented the background of adaptive arrays and optical signal processing. This chapter will present an AA processor which uses the time integrating optical correlator to provide estimates of the directions of arrival and power of up to N noise sources. The direction estimates are then used to generate complex weights such that the resulting antenna pattern has nulls of some preset depth in the desired directions. After presenting the basic form of the processor this chapter will compare a maximum likelihood estimation of source directions with this processor and present a bound on the performance of the system. Also included in this chapter are discussions of spatial angular ambiguity and resolution, an approach to efficient post processing, and some variations on the form of the TIOC for AA processing.

The Processor

The basic ideas of the TIOC for AA processing were first investigated by Casasent (Ref 1). The processor forms the correlation of the signal at the reference element (the far right element) with the signal at each of the other elements to form N correlations. For the case of a single interference source the signal at each of the

elements is simply a time delayed version of the signal at the reference element with the time delay given by (18)

$$\tau = \frac{d}{c} \sin \theta \tag{18}$$

From Table 1, the signal at the reference element from interference source k is $f_k(t)$ and the resulting signal from K sources is

$$r_0(t) = \sum_{k=1}^{K} f_k(t) \tag{19}$$

The delay for interference source k at an angle θ_k from boresight at element n of the linear array with evenly spaced elements if $n\tau_k$. The signal at element n, for n = 1,2,...,N,

$$r_n(t) = \sum_{k=1}^{K} f_k(t-n\,\tau_k) \tag{20}$$

The adaptive array processor forms the N correlations

$$R_n(\tau_D) = \int_o^T r_n(t)\; r_o(t-\tau_o)\; d\,t \tag{21}$$

Each of the correlations formed contains the following terms

$$R_n(\tau_o) = \sum_{k=1}^{K} \sum_{l=1}^{K} \int_o^T f_k(t-n\tau_k)\; f_l(t-\tau_o)\; d\,t \tag{22}$$

All of the cross terms ($k \neq 1$) are zero for sources which are either independent or not coherent. The remaining terms are each the correlation of a source signal with a time delayed version of that signal. These correlations are combined to produce $N(\theta)$ as follows

$$N(\theta) = \sum_{n=1}^{N} R_n \left(\frac{nd}{c} \sin\theta\right) \tag{23}$$

The locations of the peaks in $N(\theta)$ indicate the directions of the interference sources and the amplitude of each is proportional to the power of the corresponding noise source. The TIOC AA processor implements this approach by performing the required correlations with acousto-optic time integrating optical correlators. The structure of the processor is shown schematically in Fig. 10.

Also shown in the figure are the output correlations which would be formed for a single jammer with a rectangular waveform. Note that both positive and negative correlation delays can be produced by proper timing of the reference input $r_o(t)$. The correlation peaks line up indicating the direction of the source. The discussion so far has considered only directional noise sources and no noise in array elements or in the processor. In the next section, noise will be added to the consideration and signal characteristics will be discussed.

Maximum Likelihood Comparison

This section will show that for certain conditions, the proposed processor provides maximum likelihood estimates of the source directions. The maximum likelihood estimate of a vector of source directions will be derived and this will be shown to be equivalent to

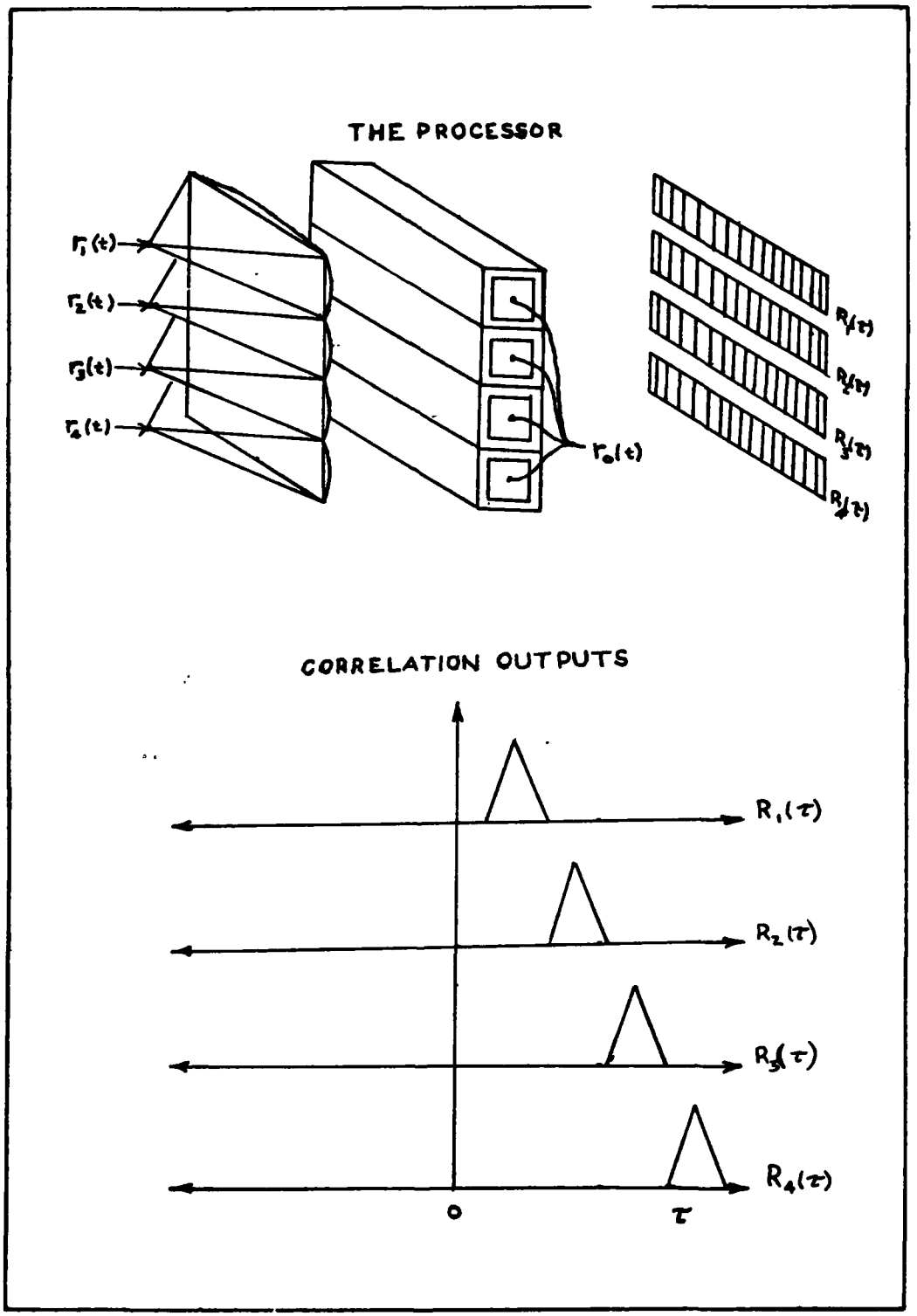

Fig 10. T10C AA Processor Structure and Output

the processor output. The directional interference sources for this derivation will be assumed to be deterministic. In addition, the sources will be teated as real signals. It is important to note here that this processor could also be implemented to operate on complex signals by performing complex correlations. The signal from the k-th source has been given as $f_k(t)$. The signals from which the estimates are to be obtained will be taken as the signals at the elements of the array $S_n(t)$, corrupted by zero mean gaussian noise sources $n_n(t)$ with variance σ_n^2, where $n_n(t)$ is the noise associated with the n-th element. The noise sources are assumed to be independent which implies that they do not derive from directional noise sources. As can be seen from Fig. 11, which shows two sources and a three element array, the signal $r_n(t)$ from the n-th element has the form

$$r_n(t) = \sum_{k=1}^{K} f_k(t - n\tau_k) + n_n(t) \qquad (24)$$

If $r_n(t)$ is represented by $\underline{I}$ time samples where $r_{n,i} = r_n(t_i)$ and the outputs from all of the elements are combined to form the vector $\underline{r}$ which has the form

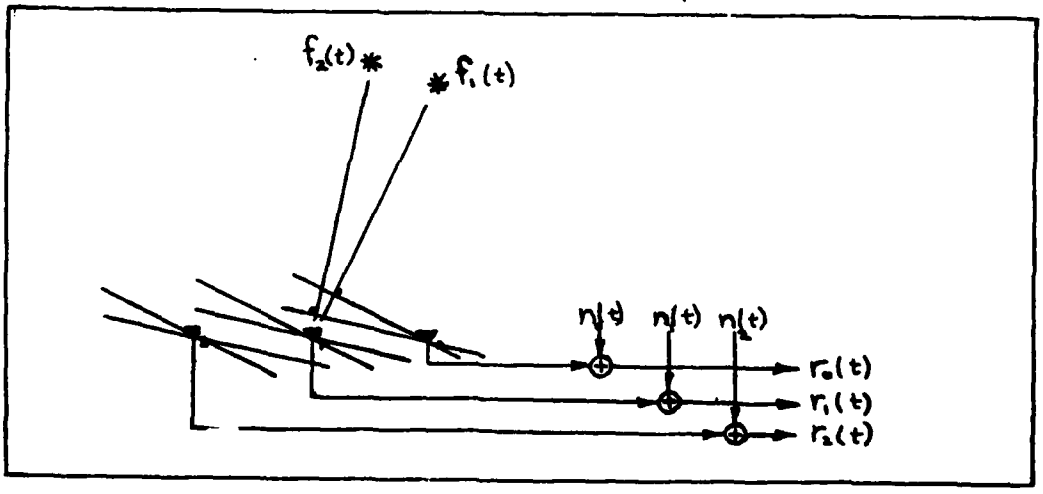

Fig. 11. Array Signal Structure

$$\underline{r} = \begin{bmatrix} r_{0,1} \\ \vdots \\ r_{0,I} \\ r_{1,1} \\ \vdots \end{bmatrix} \cdots \begin{bmatrix} \vdots \\ r_{N-1,I} \\ r_{N,1} \\ \vdots \\ r_{N,I} \end{bmatrix} \tag{25}$$

for an array of N + 1 elements. The desired directions can be derived directly from the associated time delays so we will form an estimate for the vector $\underline{\tau}$ whose elements are the K element to element time delays τ_k. The condition probability density of $\underline{r}$ given $\underline{\tau}$ is

$$p(\underline{r}/\underline{\tau}) = \prod_{n=0}^{N} \prod_{i=1}^{I} \left(\frac{1}{2\pi T_n}\right)^{\frac{1}{2}} \exp\left[- \frac{\{r_{n,i} - \sum_{k=1}^{K} f_k(t_i - n\tau_k)\}^2}{2\sigma_n^2} \right] P_r(p_k) \tag{26}$$

The maximum likelihood estimate of $\underline{\tau}$ is the vector $\hat{\underline{\tau}}$ which maximizes the likelihood function $\Lambda(\underline{\tau}) = \ln (p\ (\underline{r}/\underline{\tau}))$. This is equivalent to minimizing the magnitude of the exponent.

After dropping the denominator which has no dependence on $\underline{\tau}$, the quantity to be minimized is

$$\sum_{n=0}^{N} \sum_{i=1}^{I} \left\{ r_{n,i} - \sum_{k=1}^{K} f_k(t_i - n\tau_k) \right\}^2 \tag{27}$$

After performing the square the resulting terms are

$$\sum_{n=0}^{N} \sum_{i-1}^{I} r_{n,i}^2 \tag{28}$$

$$-2 \sum_{n=0}^{N} \sum_{i=1}^{I} r_{n,i} \sum_{k=1}^{K} f_k (t_i - n\tau_k) \tag{29a}$$

$$\sum_{n=0}^{N} \sum_{i=1}^{I} \left| \sum_{k=1}^{K} f_k(t_i - n\tau_k) \right|^2 \tag{29b}$$

The first term does not depend on $\underline{\tau}$ so it will not affect the minimization. Terms (29a and 29b) can be rewritten with the summation over time replaced by an integral.

$$-\sum_{n=0}^{N} 2 \int_{o}^{T} r_n(t) \sum_{k=1}^{K} f_k(t - n\tau_k)\, dt \tag{30a}$$

$$\sum_{n=0}^{N} \int_{o}^{T} \sum_{k=1}^{K} f_k(t - n\tau_k)^2\, dt \tag{30b}$$

At this point, it is assumed that the integral of the cross products in (30) is not dependent on $\underline{\tau}$. This condition is generally satisfied if the sources are not coherent with each other. Given this assumption and noting that the integral of the squared terms does not depend on $\underline{\tau}$, it is observed that maximizing the likelihood function can be accomplished by maximizing the magnitude of (30a). Noting that the n equals zero term does not depend on $\underline{\tau}$. The estimate $\underline{\tau}$ is defined as $\underline{\hat{\tau}}$ such that

$$\sum_{n=1}^{N} \int_{o}^{T} r_n(t) \sum_{k=1}^{K} f_k(t - n\tau_k) dt \tag{31}$$

is maximized. This can be compared to the correlations formed by the

proposed processor as was given in (22)

$$R_n(\tau_D) = \int_0^T r_n(t)\, r_o(t-\tau_D)\, dt \tag{32}$$

if r_o is replaced by (24)

$$R_n(\tau_D) = \int_0^T r_n(t) \left| \sum_{k=1}^{K} f_k(t-\tau_D) + n_o(t) \right| dt \tag{33}$$

Replacing τ_D by $n\,\tau_D$ to scale each correlation as indicated in (23) and summing over n the TIOC produces

$$N(\theta) = \sum_{n=1}^{N} \int_0^T r_n(t) \left| \sum_{k=1}^{K} f_k(t-n\tau_D) + n_o(t-n\tau_o) \right| dt \tag{34}$$

where the dependence of τ_D on θ is given by (19).

If the noise $n_o(t)$ is uncorrelated with the directional noise sources (or assuming high signal-to-noise) it is clear that determining the values of τ_D which maximize $N(\theta)$ is equivalent to maximizing the likelihood function. It is to be noted that maximum likelihood requires that (33) be maximized independently for each source k and that $N(\theta)$ sets all τ_k values equal to τ_D and find k values which maximize N. The operations are, in fact, equivalent for wideband or incoherent sources. If the sources are replaced by random sources derivation of the maximum likelihood estimate is mathematically difficult; however, if the integration is long enough the correlation operation produces a good estimate of the covarience and it is apparent that for wideband sources the peaks produced in $N(\theta)$ provide estimates of the directions of the sources.

Cramer-Rao Bound

To quantify the performance of the adaptive array processor, it is helpful to investigate the Cramer-Rao bound on the variance of the estimate produced by maximum likelihood estimation. The bound for the real signal case which has been assumed to this point is derived here. The derivation for complex signals would be similar to that given by Whalen (Ref 24:337-342) for the variance of a time of arrival estimator for radar signals. The Cramer-Rao bound is given by

$$\{\text{var } \underline{\hat{\tau}}/\underline{\tau}\} \geq \left[E\{\frac{\partial^2 \ln(p(\underline{r}/\underline{\tau}))}{\partial \underline{\tau}^2}\}\right]^{-1} \tag{35}$$

It was shown previously that the log likelihood function was proportional to

$$\ln(p(\underline{r}/\tau)) \propto \sum_{n=1}^{N} \{\ln (\frac{2}{\pi\sigma_n})^{\frac{1}{2}} + \frac{1}{\sigma_n^2}\int_o^T r_n(t) \sum_{k=1}^{K} f_k(t-n\tau_k)\, dt\} \tag{36}$$

To allow the Cramer-Rao bound to be written without the expectation operator, a high signal-to-noise ratio will be assumed. Assuming also, as before, that the cross correlations of the interference sources are not dependent of τ the bound can be written as

$$\text{var } \{\underline{\hat{\tau}}/\underline{\tau}\} > \left[\sum_{n=1}^{N} \frac{\partial^2}{\partial \underline{\tau}^2} \frac{1}{\sigma_n^2}\int_o^T \sum_{k=1}^{K} f_k^2 (t-n\tau_k)\, dt\right]^{-1} \tag{37}$$

remembering that the derivative is evaluated at the true value of $\underline{\tau}$. If f(t) has a Fourier transform given by $F(j\omega)$ then

$$f_k(t) = \frac{1}{2\pi} \int_{-\infty}^{\infty} F_k(j\omega)\, e^{j\omega t}\, d\omega \tag{38}$$

and by Parseval's theorem

$$\int_0^T f_k^2\,(t-n\tau_k)\, dt \triangleq \frac{1}{2\pi} \int_{-\infty}^{\infty} |F_k(j\omega)|^2\, d\omega \tag{39}$$

assuming that nearly all of the energy in $f_k(t-n\tau_k)$ is contained in the interval from 0 to T. The derivative is then easily evaluated given that the Fourier transform of $\partial^2(x(t))/\partial\underline{\tau}^2$ is $-\omega^2 X(j\omega)$. The resulting bound on the variance is

$$\text{var}\,\{\underline{\hat{\tau}}/\underline{\tau}\} \geq \left[\sum_{n=1}^{N}\sum_{k=1}^{K} \frac{1}{\sigma_n^2}\,\frac{1}{2\pi}\int_{-\infty}^{\infty} \omega^2 |M_k(j\omega)|^2\, d\omega\right]^{-1} \tag{40}$$

The energy in the kth signal is

$$E_k = \frac{1}{2\pi} \int_{-\infty}^{\infty} |M_k(j\omega)|^2\, d\omega \tag{41}$$

The noise variance can be replaced by $N_n/2$ and substituting (41) into (40) yields

$$\text{var}\,\{\underline{\hat{\tau}}/\underline{\tau}\} \geq \left[\sum_{n=1}^{N}\sum_{k=1}^{K} \frac{2E_k}{N_n}\,\beta_k^2\right]^{-1} \tag{42}$$

where β_k is a measure of bandwidth of the k-th source defined by

$$\beta_k^2 = \frac{\int_{-\infty}^{\infty} \omega^2 \, M(j\omega)^{\,2} \, d\omega}{\int_{-\infty}^{\infty} |M(j\omega)| \, d\,\omega} \tag{43}$$

as given by Whalen (Ref 24:339). This bandwidth measure is the second moment of the signal spectrum about $\omega = 0$. Whalen shows that a similar problem with a narrowband signal with random phase yields similar results with β redefined as the second moment of the signal spectrum about the mean of the spectrum (Ref 24:342).

The important conclusions to be drawn from the bound as expressed in (42) are the improvements in the estimate to be gained from higher signal-to-noise and larger numbers of correlations N. Perhaps even more important, is the observation that the performance of the estimator and thus the processor under consideration is dependent upon large bandwidth signals.

Ambiguity

This section analyzes the ambiguity present in the output of the TIOC AA porcessor. The ambiguity in detection of the angle at which an interference source is located is dependent on the parameters of the AA and on the characteristics of the interference source. The symmetry of the linear array limits the range of angles to 90 degrees either side of boresight (a source detected at 37 degrees may be at 37 or 143 degrees). To understand the other limitations, it is easiest to first look at the ambiguity in each of the correlations and then translate this back to $N(\theta)$. For a completely incoherent source (this implies infinite bandwidth) only one correlation peak is produced no matter what range over

which the correlation delay is varied. Most sources of radiation at frequencies less than several gigahertz are highly coherent so their autocorrelation functions are periodic. A source which is periodic with period T_s and has a coherence time greater than the correlation time will have an autocorrelation which is periodic on the delay τ_D. If the distance between the elements for which the correlation is produced is greater than the wavelength $\lambda = cT_s$, of the source then more than one correlation peak will be produced in the range over τ_D which corresponds to the otherwise unambiguous range of θ from -90 to 90 degrees. This is illustrated in Fig. 12 for an array of five elements spaced $\lambda/2$ apart. The source for this example is a pulse train with period T_s. The dashed line indicates the delays associated with 90 degrees and the correlations are shown for a source at 90 degrees. There is no ambiguity beyond that caused by symmetry for $R_1(\tau_D)$ but as can be seen in the figure, numerous peaks are present between -90 degrees and 90 degrees for the other correlations. For no ambiguity to be added by the periodicity of the correlation the separation between the reference element and the element with which the correlation is performed must be less than one half of a wavelength. The maximum unambiguous range for a source at a given angle is not the same for sources at different angles. The maximum unambiguous range in τ_D is $\pm T_s$ and (1) can be used to find the corresponding range of angles. This range which corresponds to $\tau_D \pm T_s$ is

$$\Delta\theta = \sin^{-1}\left\{\frac{c}{nd}(\tau+T_s)\right\} - \sin^{-1}\left\{\frac{c}{nd}(\tau- T_s)\right\} \qquad (40)$$

The effect of this ambiguity is reduced in the TIOC for AA by the addition of several correlations together. The locations of the

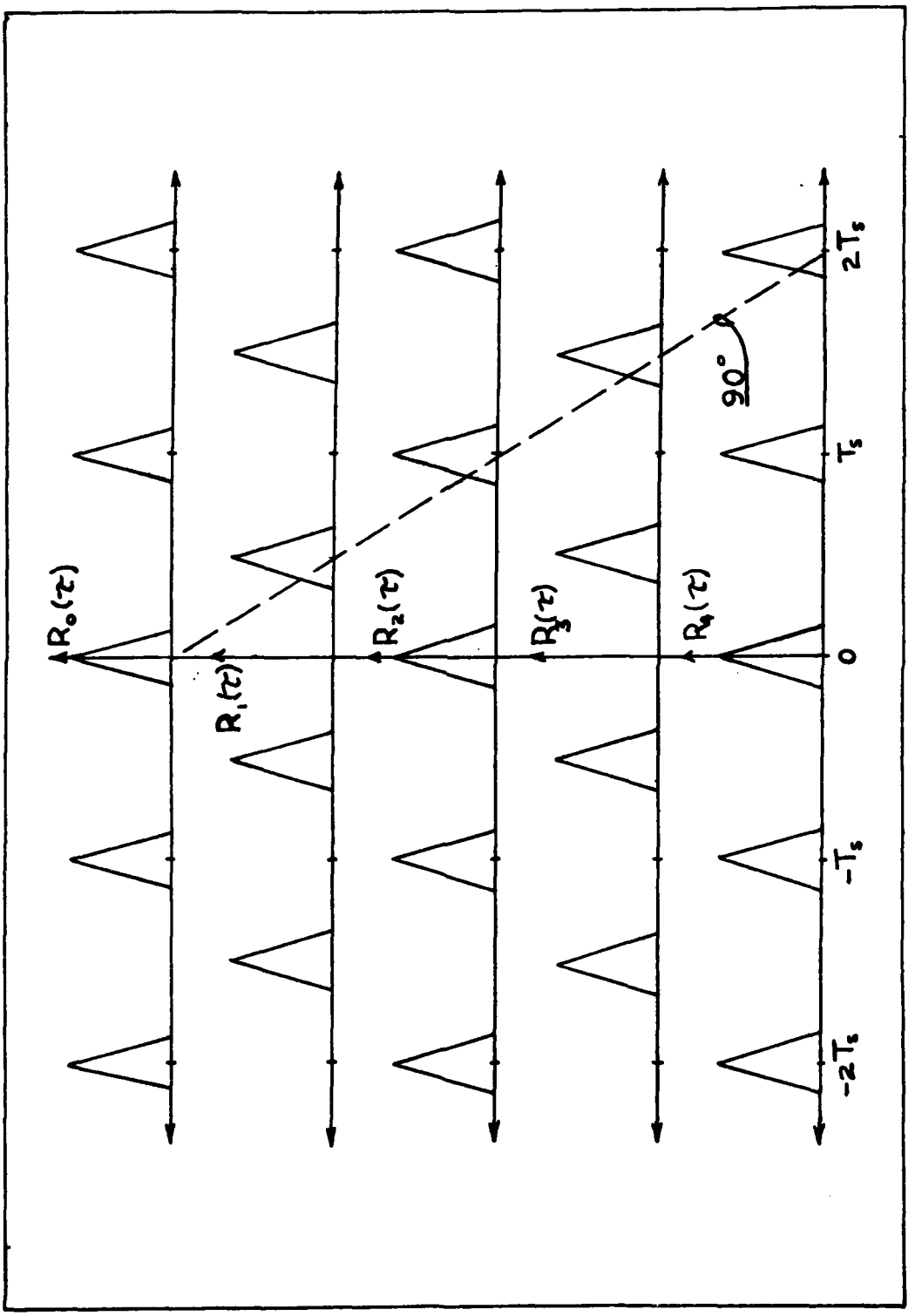

Fig. 12. Ambiguity in Array Output

ambiguous peaks do not line up for angles other than the correct peaks.

Resolution

The resolution of this system is limited by the implementation with optical processing and by the characteristics of the signals being detected. The limit imposed by the implementation is the finite resolution of the correlation at the detectors as discussed in Chapter IV. With existing devices this limitation restricts the range of applications. Casasent discusses this limitation as applied to adaptive phased array radar (Ref 1:33). The resolution required in the AO cells which have set time windows of .5 to 40 μsec is determined by the velocity of propagation of the interference signal. For an AO cell with a time window of 1 μsec and a time bandwidth product of 1000 the smallest resolvable time delay is 1 μsec To provide 100 resolvable locations from boresight to 90 degrees would require an element spacing of .3 meters. Casasent suggests elimination of this limitation on resolution by using an adjunct antenna element 17.3 meters from the reference element. This solution, however, could lead to ambiguity as discussed in the last section if the interference sources are coherent over a period of time comparable to the arrival delay of the signal from the adjunct element to the reference element. Addition of several more adjunct elements would decrease the effects of these ambiguous correlation peaks as indicated in the last section. It should be noted here that simply increasing the element to element spacing for the linear array is undersirable because of resulting null placement limitations.

The other factor contributing to resolution limitations is the width of the correlation peak which is related to the bandwidth of the

interference source as shown in Chapter III. For simplicity, the interference source once again will be assumed to be a pulse of duration T_s and bandwidth $B \triangleq 1/2\ T_s$. The correlation peak width is taken as $W_s \triangleq 1/B$. The relation between the correlation delay and angle is given once again by

$$\tau = -\frac{d}{c}\ \sin\theta \tag{45}$$

The effect of this nonlinear transformation is that the resolution at different angles from boresight varies greatly. The relationship for the width of the peak occurring in $N(\theta)$ is

$$\Delta\theta = \sin^{-1}\{\frac{c}{d}\ (\tau_s + \frac{W}{2})\}\ -\ \sin^{-1}\{\frac{c}{d}\ (\tau_s + \frac{W}{2}\ )\} \tag{46}$$

For an element separation d of 10 meters and a pulsewidth of 1 nsec from a source at 10 degrees the angle $\Delta\theta$ is 1.75 degrees. For the same source at 90 degrees the angle $\Delta\theta$ is 19.9 degrees. The width of a peak at angle θ is given by the approximate relationship

$$\Delta\theta \triangleq \frac{\Delta\theta\text{boresight}}{\cos(\theta)} \tag{47}$$

Post Processing

The interference source directions provided by this processor must be efficiently utilized to generate the complex weight values which produce nulls in those directions. The antenna response $B(\theta)$ resulting from a given set of weights was given in (3) and is repeated here

$$B(\theta) = \sum_{n=1}^{N} W_n \exp(j \frac{2\pi n d f}{c} \sin\theta) \quad (48)$$

where f is the frequency for which $B(\theta)$ is valid. Casasent notes that this is a discrete Fourier transform for the case where θ is replaced by the source angles θ_k and f by the frequencies of the sources f_k (Ref 1:62). This approach to computing the weight vector $\underline{W}$ is not, however, applicable if the sources are at different frequencies.

Another approach to determining the weight vector is to set up a system of linear equations. Each equation determines the response of the array for a given direction at a particular frequency. For an N+1 element array N+1 equations must be set up to completely determine the weights. A matrix $\underline{P}$ is formed whose elements are

$$P_{m,n} = \exp(j\ 2\ \pi n f_m\ sin\ \theta_m) \quad (49)$$

The vector matrix equation

$$\underline{B} = \underline{P}\ \underline{W} \quad (50)$$

must then be solved. To maintain a desired response at boresight to the desired signal at frequency f_1 the first row of P is defined as

$$P_{1,n} = 1 \quad \text{for} \quad n = 1, N+1 \quad (51)$$

and B_1 is defined as the desired response at boresight. The interference source directions θ_m, and frequencies f_m, are used to complete $\underline{P}$ and to provide nulls at these angles and frequencies. The remaining elements of $\underline{B}$ are set equal to zero. The resulting vector matrix equation for $\underline{W}$

$$\underline{W} = \underline{P}^{-1}\,\underline{B} \tag{52}$$

can be solved by finding only the first column of the $\underline{P}$ matrix. This is true because the vector $\underline{B}$ has only one nonzero element which is its first entry. The special way in which $\underline{P}$ is formed produces an array with a number of unique properties. It seems likely that if these properties can be put to use, an efficient solution of the vector matrix equation can be found. Casasent suggests a technique for solving this system of equations using projection mapping techniques (Ref 1:66).

Variations

This section will briefly present some variations on the basic form of the processor which extend its capabilities or enhance its implementation. The first variation to be discussed is suggested by Casasent to generate the source frequency information which would be needed to place nulls at specific frequencies as discussed in the previous section. The processor proposed uses time and space integrating concepts within the same processor to produce the correlation output already discussed and produces an estimate of the noise power contained different frequency bands by correlating a bandpass filtered signal with the original signal. The filtering operation is performed using the Fourier transform property of light propagation as discussed in Chapter II.

One other variation on the basic form of the processor is shown in Fig. 13. This processor uses multiple sources with a single acousto-optic cell to generate the desired correlations. The sources are at different wavelengths λ_1, λ_2, and λ_3 and are modulated by

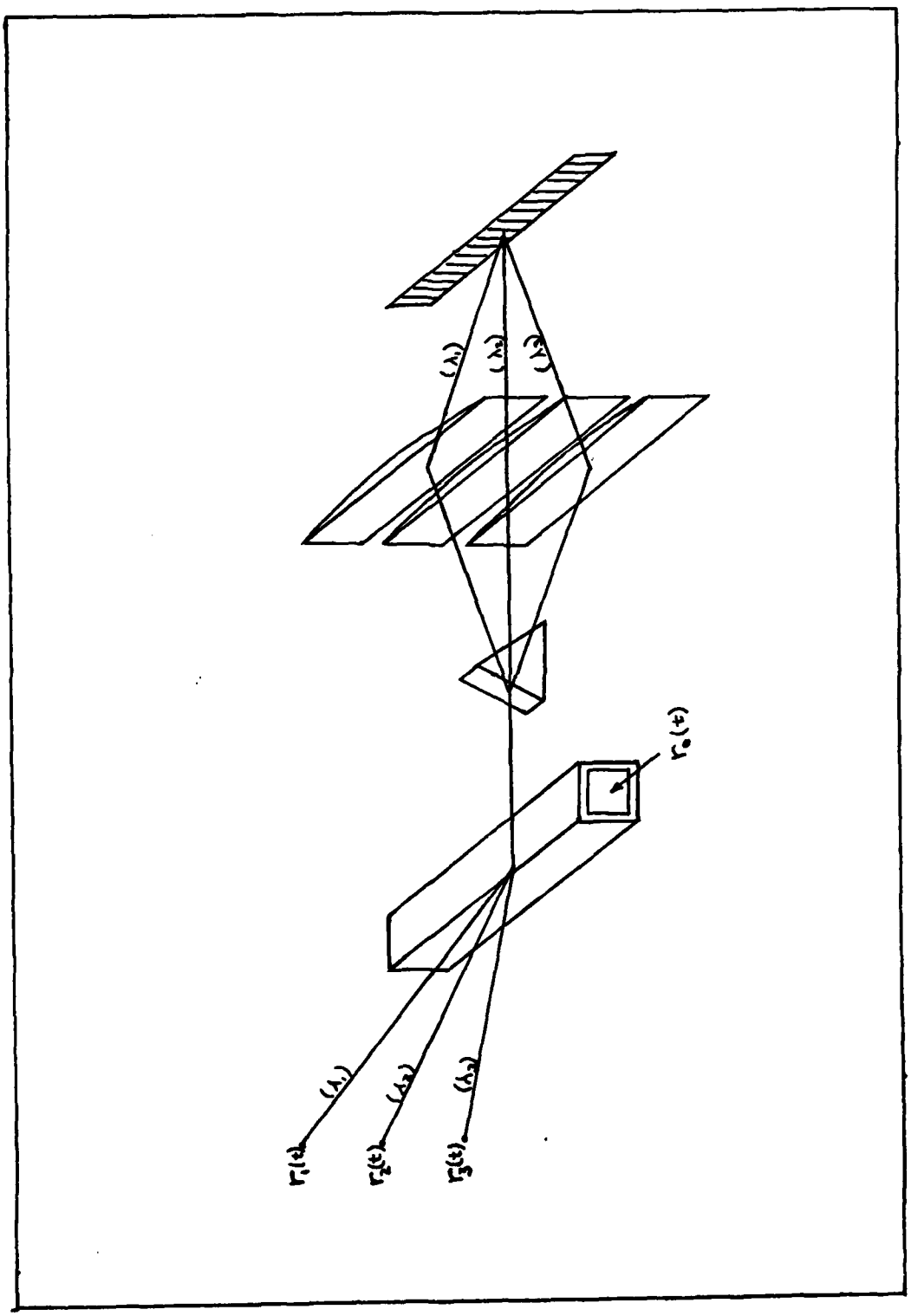

Fig. 13. Multiple Source-Single Cell Processor

the signals $r_1(t)$, $r_2(t)$ and $r_3(t)$. The signal from the reference element $r_o(t)$, is used to modulate each of these and a prism is used to separate the resulting outputs. The products $r_o(t-\tau)\, r_1(t)$, $r_o(t-\tau)r_2(t)$, and $r_o(t-\tau)r_3(t)$ are then imaged with different magnifications onto the same detector array. The output then has the form

$$R(\tau) = \int_o^T r_o(t-\tau_1)r_1(t) + r_o(t-\tau_2)r_2(t) + r_o(t-\tau_3)r_3(t)\, dt \qquad (53)$$

If the lens are specified correctly

$$\tau_3 = 3\,\tau_1 \quad , \text{ and}$$

$$\tau_2 = 2\,\tau_1 \qquad (54)$$

This processor then provides a sum of three correlations with the advantage of requiring only one detector array. With this implementation, the detection noises due to thermal sources, dark noise, quantization error, and readout error are added to the output only once rather than 3 times as would be the case with 3 separate correlators.

VI. Simulation Results and Conclusions

Introduction

The complex nature of the relationship of the characteristics of the signal environment and the parameters of the processor to the performance of the system prompted the development of a computer program capable of simulating the processor under consideration. The results of that effort are presented in this chapter. The simulation produced results which confirm the conclusions drawn in Chapter V concerning resolution and ambiguity. Conclusions concerning a comparison of these results to other adaptive array processors will then be given, followed by some suggestions for future research in this area.

Simulation Results

Simulation of the TIOC processor and its environment was complicated by the multitude of processor and signal parameters. The program was constructed using four subroutines called by a main program. A listing of the program is included in the Appendix. The first subroutine was adapted from a similar subroutine developed by Casasent (Ref 1:37). This routine, labeled ARRAY, generates the composite signal present at each element of an arbitrary size linear array of equally spaced elements. Any number of interference sources may be

simulated. Although only sinusoidal and periodic rectangular pulse signals were included in the simulation runs, any signal source for which code can be written to represent a function of time could be substituted into the routine. The output of the routine is a matrix containing a vector of time samples representing the signal at each element of the array.

The next routine, labeled CORR, performs the correlation of the signal at the reference element with the signal at each of the remaining elements in the array. The output is a matrix containing vectors of correlation values at different correlation delays for each of the correlations formed.

The ANGL routine accepts the correlation outputs and generates values for $N(\theta)$ at every one-half degree from zero to ninety degrees. These values are then analyzed to identify the maximum values corresponding to the angle estimates of the source directions. A parameter was introduced into this routine called RES. To help prevent identification of several points associated with the same peak only those points whose angular distances from previously identified points are greater than the self-imposed resolution limit, RES, are retained as valid points.

The final routine, WAITS, accepts the angle estimates generated by ANGL and determines complex weights for each element of the array by solving a system of complex linear equations. The system of equations is solved to generate a specified response at boresight and at each of the estimated source angles. An IMSL routine LEQT1C was used to provide the solutions for the system of equations. The depth of the nulls provided by the computed weights is limited only by the accuracy of LEQT1C. WAITS uses the computed weights to determine the

antenna pattern using (3).

Simulation runs were performed for both sinusoidal and periodic rectangular pulse interference sources. As predicted by the analysis in Chapter V, the resolution for the sinusoidal input is very poor due to its narrow bandwidth. The processor output for $N(\theta)$ with one cosinusoidal source at 17 degrees is shown in Fig. 14 . Poor resolution

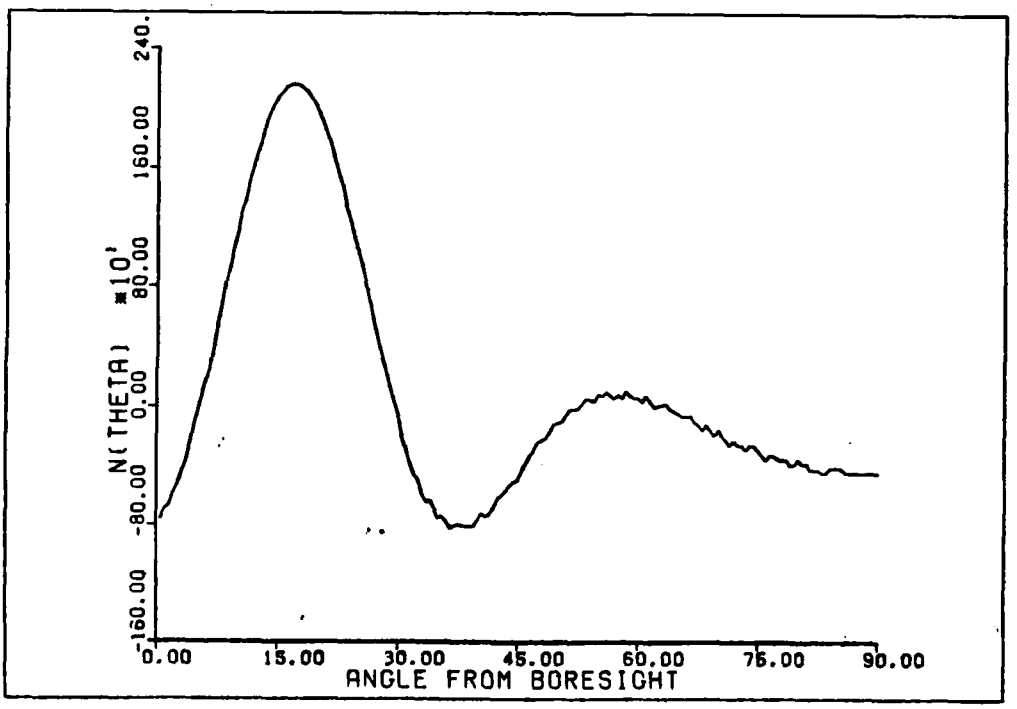

Fig. 14. Simulation Output for One Sinusoidal Input

and ambiguity as discussed in Chapter V degrade the processor output for the sinusoidal input so greatly that correct angle estimates were produced by the simulation runs for only the single source case. This case, as well as the other discussed here, were performed for a five element linear array with a one-half wavelength element spacing. Ninety sample points were produced for each period for a total of 1000 points at each element. The integration time was set at 360 points

corresponding to four periods of the input waveform. The range of correlation delays was set at 400 or just over four periods. In all cases, the period of the interference sources were equal to the frequency of operation of the array.

A rectangular period pulse train signal was also used as an interference source. This model for the source allows easy variation of the bandwidth by varying the fraction of the period over which the pulse is present. Shown in Fig. 15 are the results obtained for a source

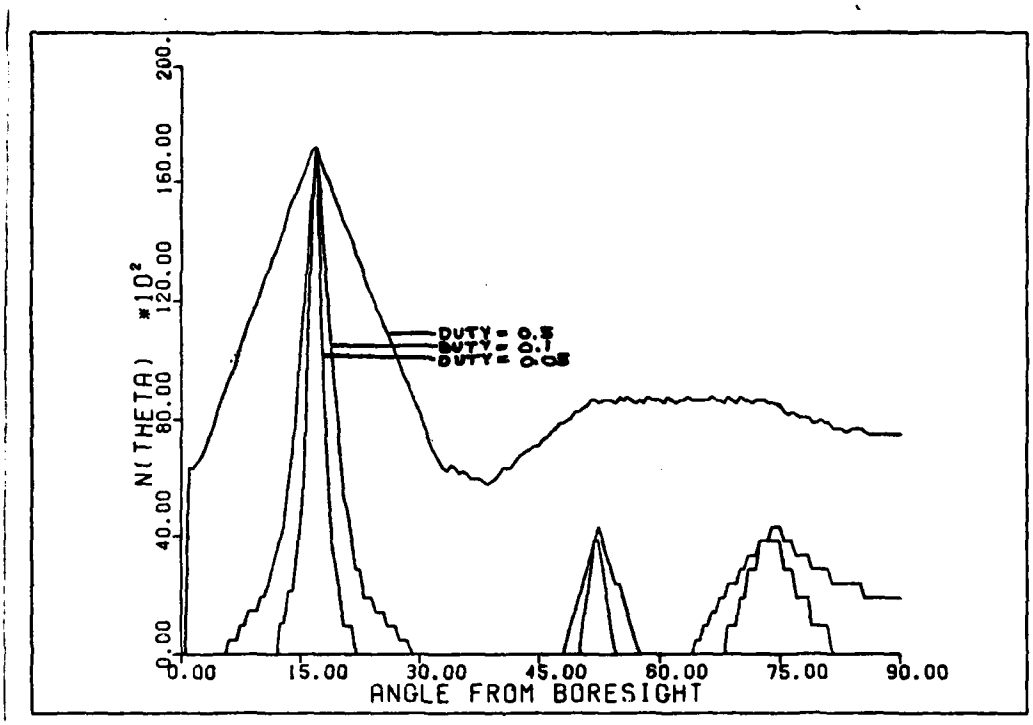

Fig. 15. Simulation Output for Rectangular pulse Train Inputs

at 17 degrees with rectangular pulses. The widest peak at 17 degrees corresponds to pulse train with pulses one-half of the period length which will be referred to here as a duty of 0.5. The other peaks at 17 degrees correspond to duties of 0.1 and 0.05 for the intermediate and narrowest peaks, respectively. Note that these sources are very

wideband with bandwidths of approximately 4,20, and 40 times the operation frequency of the array. These bandwidths are obviously very high but they are illustrative of the wide bandwidths needed for this element spacing to achieve good resolution. As predicted in Chapter V, ambiguous pulses are also present at 52.0 and 72.5 degrees. Due to the fact that the results from four correlations were combined, the false peaks are lower than the correct peaks. Note that the amplitude of each of the sources used for this example was adjusted to provide the same energy and thus, about the same peak height in the output.

To illustrate the reduced resolution at angles near ninety degrees, the plot shown in Fig. 16 was produced. This is the simulation output for a periodic pulse train source at ninety degrees with a duty of 0.1.

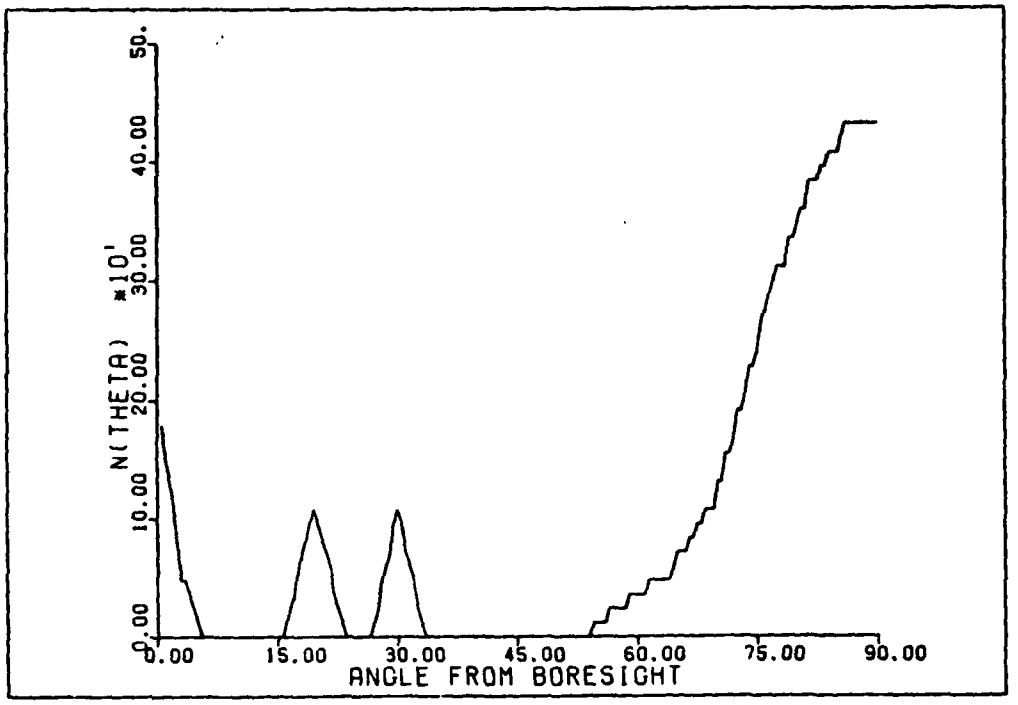

Fig. 16. Simulation Output for Source at 90 Degrees

Wideband inputs allowed the simulation program to be run for multiple source angles. Fig. 17 shows the processor output for four period pulse train sources, each with a duty of 0.2 at angles of 17, 45, 53, and 61 degrees. The peak detection routine identified peaks at 17, 45, 53, and 62 degrees and the WAITS routine generated the weights in Fig. 17b. It is to be noted here that the depth of the nulls in the antenna response could be specified at any value limited only by the hardware used to implement the procedure.

Simulation of a great number of other cases was also performed, however, the plots which have been presented here illustrate all of the significant results. These results included confirming the increase in resolution with wideband signals, the differences in resolution at different angles, the presence of ambiguous peaks for periodic sources, and the ability of the processor to recognize multiple sources and to produce the proper weights to null these sources.

Processor Performance Evaluation

Based upon the adaptive array background as discussed in Chapter 22, the TIOC for AA processing approach can be evaluated using the results of the investigation of time integrating optical correlators and the analysis of the characteristics of this type of processor as presented in Chapter IV and V. First of all, it is important to note that the processing approach which has been discussed is a higher order method in contrast to mose of the algorithm which uses a steepest descent approach (first order). This allows the processor to adapt in a single

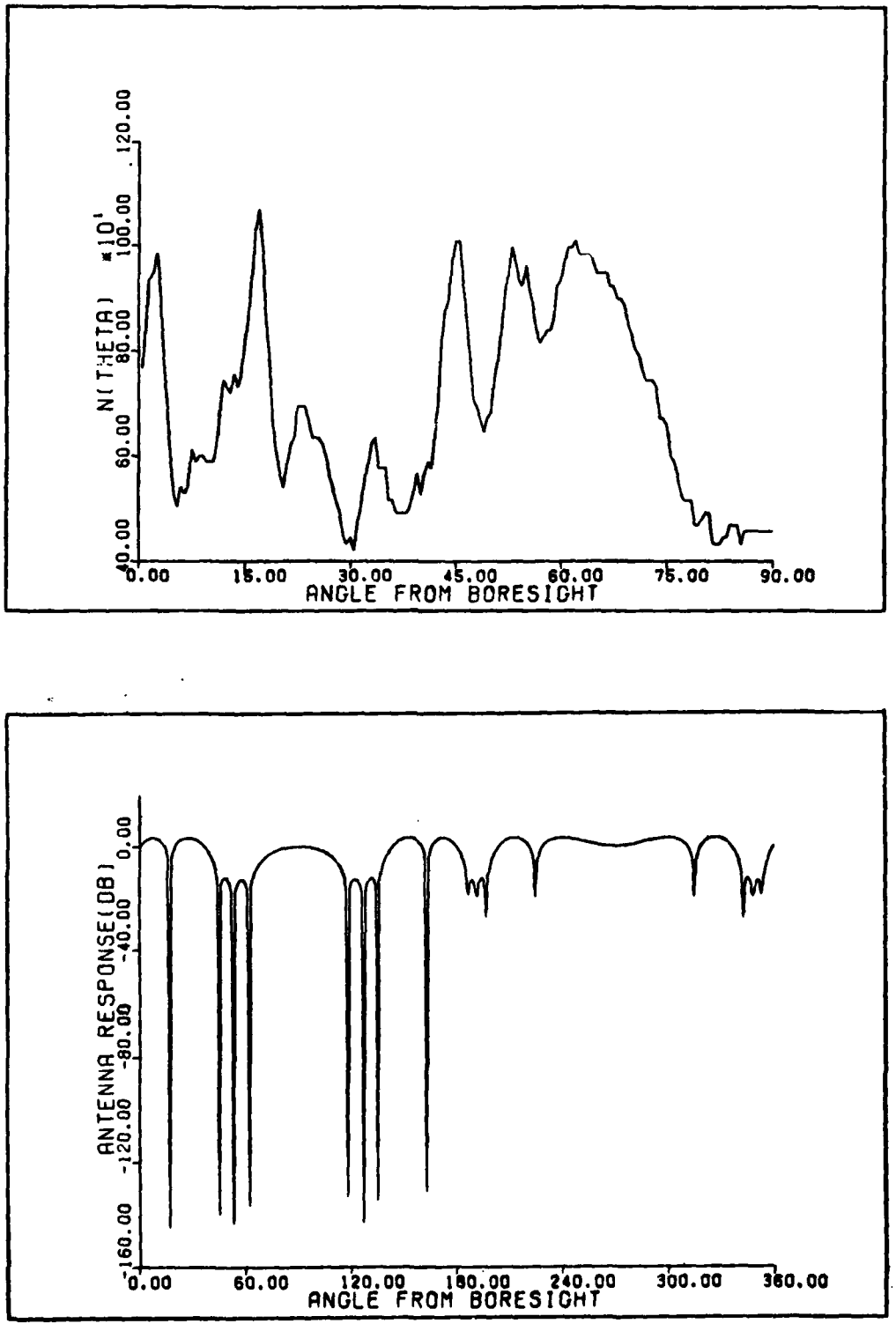

Fig. 17. Simulation Output and Resulting Antenna Response for Four Sources

processing cycle rather than approaching the optimum in small steps. Another point in favor of this system is its flexibility. As discussed, the processor assumes a known direction of arrival, however, the system could easily be modified to acquire the signal based on correlation with a signal having the desired signal characteristics. The processor could obviously also be operated in an all signal suppression mode. As discussed briefly in Chapter V, addition of spectrum analysis to the system could provide the added flexibility of producing nulls at any specified frequencies. The depth of the nulls, as well as the width or frequency range, is dependent only on the hardware used to implement the weights.

The problems associated with this processor are, however, numerous. It has been shown in Chapter V that the processor is the optimum estimator of source angle. The conditions imposed on the signal enviornment, however, limit the applicability of these results. These conditions were that the interference sources were incoherent over the integration time thus producing nonperiodic correlations and that multiple sources were uncorrelated with each other. As shown by the Cramer-Rao bound and the discussion on resolution, performance of the system is also highly dependent on large bandwidth signals. The effects of periodic signals which are coherent over the integration time was discussed in the section on ambiguity and the ambiguous peaks were observed in the simulations. The poor resolution created by narrow bandwidth signals was shown by simulating a sinusoidal input. The effects of correlated sources have not been analyzed explicitly here. However, depending upon the degree to which the sources are correlated,

it is obvious that additional peaks would result in the correlation output. The plot in Fig. 17 shows many extra peaks, some of which are due to the periodicity of the correlations and some ow which are due to cross-correlations between the sources.

In addition to these limitations imposed by the array environment, implementation of the processor with time-integrating optical correlators sets further limits on resolution. Large array element separations are required to overcome this resolution limit. The dynamic range of the processor is also limited by the numerous noise sources and bias levels included in the correlator output.

Taking into consideration all of these factors, it appears that for certain applications the TIOC for AA processing offers possibilities for flexibility and fast accurate performance. The limitations discussed suggest, however, that without improvements in the resolution of the time integrating optical correlator the range of applications is very limited.

Future Investigation

There are many possibilities for further investigations related to the TIOC for AA processing. Simulations of different types of sources as well as the addition of nondirectional noise could be added and various element spacings could be simulated. The similarity of this processor to radar lies in the problem of detecting time of arrival by correlation. Investigation of signal processing techniques used to enhance radar performance should be made to determine applicability to this processor. Some form of angle gating (corresponding to range gating for radar) might be possible to improve performance of the system.

Summary

This thesis has investigated the application of optical signal processing to adaptive array processing. Adaptive array processing was investigated and the repeated use of correlation in the common algorithms led to the decision to concentrate the study of optical signal processing in the area of optical correlators. The characteristics of both spatial integrating and time integrating correlators were analyzed and selection of the time integrating form was made based upon the signal processing needs of the adaptive array and the capabilities of each type of processor. An adaptive array processor which was first investigated by Casasent (Ref. 1 and 2) was presented and this processor was compared to an optimum processor for a given set of conditions. The Cramer-Rao bound on the performance of this adaptive array processor was derived. Ambiguity in the output and the resolution of the system were discussed and an approach to post processing was presented. Many variations on this processor both in its approach and its implementation are possible and two variations were discussed in Chapter V. Simulation of the processor and its environment was accomplished for a number of variations and the results for several cases have been included in this chapter. An evaluation of limitations on the performance of the time integrating optical correlator for adaptive array processing for different applications was discussed and it was concluded that in many situations its performance would not be satisfactory. The positive points in this evaluation suggest, however, that for certain environments the system would perform well and several areas for future study of this processor have been indicated.

Bibliography

1. Casasent, David. Optical Processing for Adaptive Phased Array Radar. RADC-TR-81-152. Carnegie-Mellon University, 1981. (AD-A 105124).

2. Casasent, David. Optical Processing for Adaptive Phased Array Radars. RADC-TR-80-53. Carnegie-Mellon University, 1980. (AD-A086964).

3. Hendrickson, Richard L. Adaptive Array Antenna Technology, MTR5270. MITRE Corporation, August 1976. (ADB017908).

4. Gabriel, William F. "Adaptive Arrays - An Introduction," Proceedings of the IEEE, 64:239-272 (February 1976).

5. Widrow, B., P.E. Montley, L.J. Griffeths, and B.B. Goode. "Adaptive Antenna Systems," Proceedings of the IEEE, 55: 2143-2159.

6. Baird, Charles A., Jr., George G. Rossweiler, Charles L. Zahm and G. Patrick Martin. Adaptive Processing for Antenna Arrays. Radiation Incorporated, Melbourne, Florida, July 1972. (AD-748220).

7. Torrieri, Don J. Principles of Military Communication Systems. Artech House Inc., Dedham Ma., 1981.

8. Applebaum, Sidney P. "Adaptive Arrays," IEEE Transactions on Antennas and Propagation, AP-24: 585-599.

9. Goodman, Joseph W. Introduction to Fourier Optics, San Francisco: McGraw-Hill Book Co., 1968.

10. Casasent, David. "Spatial Light Modulators and Their Uses in Optical Data Processing," SPIE, 128: 56-67 (1977).

11. Sprague, Robert A. "A Review of Acousto-Optic Signal Correlators," SPIE, 90: 136-147 (1976).

12. Rhodes, William T. "Acousto-Optic Signal Processing: Convolution and Correlations," Proceedings of the IEEE, 69: 65-79 (January 1981).

13. Guilfoyle, Peter S. Introduction to Acousto-Optic Signal Processing Devices, Architectures, and Applications. Tutorial T5 SPIE 26th Annual International Technical Symposium, August 22, 1982.

14. Casasent, David. "Optical Signal Processing," Electro-Optical Systems Design. 41-47. (September, 1981).

15. Korpel. Adrianus. "Acousto-Optics - A Review of the Fundamentals, "Proceedings of the IEEE, 69: 48-53 (January 1981).

16. Chang, I.C. and D.L. Hecht. "Characteristics of Acousto-Optic Devices for Signal Processors," SPIE 241: 129-138 (1980).

17. Young, Eddie H., Jr. and Shi-Kay Yao. "Design Considerations for Acousto-Optic Devices," Proceedings of the IEEE, 69: 54-63 (January 1981).

18. Hodura, Henri. "Statistics of Thermal and Laser Radiation," Proceedings of the IEEE, 53: 696-704 (July 1965).

19. Hubbard, W.M. "Utilization of Optical-Frequency Carriers for Low- and Moderate- Bandwidth Channels," The Bell System Technical Journal 52:731-765 (May-June 1973).

20. Pratt, William K. Laser Communication Systems. New York: John Wiley and Sons, 1969.

21. Ross, Douglas A. Optoelectronic Devices and Optical Imaging Techniques. London: MacMillan Press, Ltd., 1979.

22. Borsuk, Gerald M. "Photodetectors for Acousto-Optic Signal Processors, Proceedings of the IEEE, 69: 100-118 (January 1981).

23. Kellman, Peter. Time Integrating Optical Signal Processing. PhD thesis. Department of Electrical Engineering, Stanford University, June 1979.

24. Whalen, Anthony D. Detection of Signals in Noise. New York Academic Press, 1971.

APPENDIX: SIMULATION PROGRAM

```
      PROGRAM MAIN(INPUT,OUTPUT,TAPE9)
C
C     THE MAIN PROGRAM IS A UTILITY TO INITIALIZE VALUES AND
C     TO CALL THE SUBPROGRAMS
C
      DIMENSION XR(1000,5),XSOUR(20),XFREQ(20)
      DIMENSION CORR(400,5)
      REAL MANGL(20,2),T(182)
      COMPLEX Q(5,5),G(361),WAIT(5),B(5)
      COMMON /D/ NELE,PI,AD,SAMP
      COMMON /A/ XR,NPTS,NSRC,BWMOD
      COMMON /B/ T,CORR,NTAU,NCPTS,NREF
      COMMON /C/ MANGL,Q,G,WAIT,B,FREQ
      COMMON /E/ XSOUR,XFREQ
      DATA NELE,NPTS,NSRC/5,1000,4/
      DATA XR/5000(0.0)/, FREQ/1.0/
      DATA XFREQ/20(1.0)/,XSOUR/17.0,45.0,53.0,61.0,67.0/
      NREF = 1
      NTAU=400
      NCPTS=360
      B(1)=(10.0,0.0)
      B(2)=B(3)=B(4)=B(5)=(0.0,0.0)
      DATA AD/0.5/
C
      PRINT*,'NTAU IS',NTAU
      PRINT*,'NCPTS IS',NCPTS
      PRINT*,'SOURCE DIRECTIONS ARE',(XSOUR(I),I=1,NSRC)
      PRINT*,'THERE ARE ',NSRC,'SOURCES'
      PRINT*,'ANTENNA HAS ',NELE,'ELEMENTS'
      PRINT*,'ELEMENT SPACING IS ',AD,'WAVELENGTHS'
C
      CALL ARRAY
      CALL CORREL
      PRINT*,'I,J,CORR(I,J)',((I,J,CORR(I,J),I=1,400),
     1       J=2,3)
      CALL ANGL
      WRITE(*,150)(FLOAT(I)/2.0,T(I),I=1,180)
150   FORMAT(1X,2HAT,1X,F7.3,1X,8HDEGREES=,E15.9)
C
      CALL WAITS
      CALL PLOT1
      CALL PLOT2
      STOP
      END
```

```
C
C
C
      SUBROUTINE ARRAY
C
C     SUBROUTINE ARRAY COMPUTES NPTS VALUES FOR THE SIGNAL
C     AT EACH ELEMENT OF THE ARRAY DUE TO THE NSRC JAMMING
C     SOURCES.  THE ELEMENT TO ELEMENT DELAY IS FIRST FOUND
C     AND THEN THE SIGNAL AT EACH ELEMENT AT EACH TIME DUE
C     TO THAT SOURCE IS COMPUTED.  THE CONTRIBUTIONS FROM
C     ALL OF THE SOURCES ARE SUMMED AND THE RESULTS ARE
C     RETURNED IN THE ARRAY XR.
C
      DIMENSION XSOUR(20),XFREQ(20),XR(1000,5)
      COMMON /D/ NELE,PI,AD,SAMP
      COMMON /A/ XR,NPTS,NSRC,BWMOD
      COMMON /E/ XSOUR,XFREQ
      AMPL = 0.1
      PI = 3.1415926535898
      SAMP = 90.0
      DUTY=0.1
      RWAVEL = 1.0
      PRINT*,'AMPLITUDE IS ',AMPL
      PRINT*,'THERE ARE ',SAMP,'POINTS PER PERIOD'
      DO 100 IM = 1,NSRC
      PHASE = 2.0 * PI * RANF()
      PRINT*,'FOR NSRC',IM,'PHASE IS ',PHASE
      DO 90 I = 1,NPTS
      DO 80 IL = 1,NELE
      RNELE = FLOAT(IL)
      DELA=(2.0*PI*AD*(RNELE-1.0)*SIN(((XSOUR(IM))*PI)/180.0))/RWAVE
      DARG = (2.0*PI*(XFREQ(IM))*I)/SAMP + PHASE +DELA
      ISAMP=IFIX(SAMP)
      RDARG=DARG-FLOAT(IFIX(DARG/(2*PI)))*2*PI
      XAR=0.0
      IF(RDARG.GT.DUTY*2*PI)GO TO 75
      IF(RDARG.LT.0.0)PRINT*,'ERROR IN ARRAY'
      XAR=1.0
75    CONTINUE
      XR(I,IL) = XR(I,IL) + XAR
 80   CONTINUE
 90   CONTINUE
100   CONTINUE
      WRITE(*,120)((XR(I,J),J=1,5),I=1,10)
120   FORMAT(1X,10E13.7)
C
C
      RETURN
      END
```

```
C
C
C
      SUBROUTINE CORREL
C
C     SUBROUTINE CORREL PERFOMS THE CORRELATION OF
C     THE SIGNAL AT ELEMENT 1 WITH THE SIGNAL AT EACH
C     OF THE OTHER ELEMENTS.  THE INTEGRATION IS
C     PERFORMED AS THE SUM OVER NCPTS POINTS OF THE
C     PRODUCT OF THE SIGNALS.  THIS IS DONE WITH A
C     DELAY ON THE SECOND SIGNAL OF FROM 1 TO NTAU
C     POINTS.
C
      REAL T(182)
      COMMON /D/ NELE,PI,AD,SAMP
      COMMON /A/ XR,NPTS,NSRC,BWMOD
      COMMON /B/ T,CORR,NTAU,NCPTS,NREF
      REAL XR(1000,5),CORR(400,5)
      DO 60 I=1,NTAU
      DO 50 J=1,NELE
      CORR(I,J) = 0.0
 50   CONTINUE
 60   CONTINUE
C
C
C
      DO 200 IELE = 1,NELE
      IF( IELE .EQ. NREF ) GO TO 200
C
      DO 190 ITAU = 1,NTAU
      DO 180 IT = 1,NCPTS
      CORR(ITAU,IELE) = CORR(ITAU,IELE) + XR(IT,NREF)*XR(IT+ITAU,IELE
     1                  XR(IT+ITAU+IFIX(SAMP),IELE)*XR(IT,NREF) +
     2                  XR(IT+ITAU+2*IFIX(SAMP),IELE)*XR(IT,NREF)
180   CONTINUE
      IF(ITAU .GT. 5) GO TO 190
190   CONTINUE
200   CONTINUE
      RETURN
      END
```

```
      SUBROUTINE ANGL
C
C     SUBROUTINE ANGL FINDS THE CORRELATION AS A FUNCTION OF ANGLE
C     AND THEN THE SECOND PART OF THE ROUTINE, THE MANGL ROUTINE,
C     FINDS THE ANGLES AT WHICH THIS FUNCTION T(THETA) IS MAXIMUM.
C
      COMMON /D/ NELE,PI,AD,SAMP
      COMMON /B/ T,CORR,NTAU,NCPTS,NREF
      COMMON /C/ MANGL,Q,G,WAIT,B,FREQ
      REAL MANGL(20,2)
      COMPLEX Q(5,5),G(361),WAIT(5),B(5)
      DIMENSION T(182),CORR(400,5),TCOPY(182)
C     ELEMENT 1 IS REF ELEMENT
C     ASSUMES SOURCE FREQ = 1.0
      DO 200 I=1,180
      T(I) = 0.0
      DELA = 2.0*PI*AD*SIN(FLOAT(I)*PI/360.0)
      DO 100 J=2,NELE
      TAU = (FLOAT(J)-1.0)*DELA*SAMP/(2.0*PI*FREQ)
      ITAU = IFIX(FLOAT(NCPTS)/SAMP)*IFIX(SAMP) - IFIX(TAU+0.5)
      IF((ITAU .LE. 0) .OR. (ITAU .GT. NTAU)) GO TO 50
      T(I) = T(I)+CORR(ITAU,J)
      GO TO 100
 50   WRITE(*,55)ITAU,J,I
 55   FORMAT(1X,5HERROR,I5,2X,I3,2X,I3)
100   CONTINUE
200   CONTINUE
C
C     MANGL ROUTINE
C
      DO 225 I=1,2
      DO 220 J=1,NELE
      MANGL(J,I)=0.0
220   CONTINUE
225   CONTINUE
C
C
      DO 250 I=1,180
      TCOPY(I)=T(I)
250   CONTINUE
      RES = 4
      DO 500 I=1,NELE
300   CONTINUE
      MANGL(I,1)=T(1)
      MANGL(I,2)=0.5
```

```
      DO 400 J=1,180
      IF(T(J) .GT. T(INT(MANGL(I,2)*2.0))) MANGL(I,2)=FLOAT(J)/2.0
400   CONTINUE
      T(INT(MANGL(I,2)*2.0)) = -10**20
      DO 450 L=1,NELE
      IF(L.EQ.I)  GO TO 450
      IF(ABS(MANGL(I,2)-MANGL(L,2)) .GE. RES)GO TO 450
      GO TO 300
450   CONTINUE
      MANGL(I,1)=T(MANGL(I,2))
500   CONTINUE
      PRINT*,'I,MANGL(I,2)',(I,MANGL(I,2),I=1,NELE)
      PRINT*,'I,MANGL(I,1)',(I,MANGL(I,1),I=1,NELE)
      DO 600 I=1,180
      T(I)=TCOPY(I)
600   CONTINUE
      RETURN
      END
C
C
C
C
      SUBROUTINE WAITS
C
C     SUBROUTINE WAITS ACCEPTS THE MAXIMUM ANGLE
C     INFORMATION FROM THE MANGL ROUTINE AND USES
C     THESE ANGLES TO SET UP A SYSTEM OF COMPLEX
C     EQUATIONS TO PRODUCE NULLS AT THE FIRST
C     (NELE-1) ANGLES LISTED IN MANGL(I,J).  A
C     CONSTRAINT IS ACCEPTED FROM THE MAIN PROGRAM
C     IN THE B(I) VECTOR.  THIS CONSTRAINT SETS
C     THE ANTENNA RESPONSE AT BORESIGHT TO 10.0 + J0.0 .
C     THE ROUTINE CALLS AN IMSL ROUTINE 'LEQT1C'
C     WHICH SOLVES THE SYSTEM OF EQUATIONS FOR THE
C     COMPLEX WEIGHTS.  THESE WAITS ARE THEN USED
C     TO COMPUTE THE RESULTING ANTENNA RESPONSE AT
C     ANGLES FROM 1 TO 360 DEGREES.
C
      REAL WA(5),MANGL(20,2)
      COMMON /D/ NELE,PI,AD,SAMP
      COMMON /C/ MANGL,Q,G,WAIT,B,FREQ
      COMPLEX Q(5,5),G(361),WAIT(5),B(5),X
C
      DO 100 I=1,361
      G(I) = (0.0,0.0)
100   CONTINUE
C
      DO 105 I=1,NELE
      Q(1,I) = (1.0,0.0)
C
105   CONTINUE
```

```
      DO 120 I=1,NELE-1
      THETA = 2.0*PI*FREQ*SIN(MANGL(I,2)*PI/180.0)
      DO 110 J=1,NELE
      Q( I+1,J )=CMPLX( COS( FLOAT( J )*THETA),SIN( FLOAT( J )*THETA
110   CONTINUE
120   CONTINUE
C
      PRINT*,'Q MATRIX'
      PRINT*,((' I,J,Q(I,J)= ',I,J,Q(I,J),I=1,5),J=1,5)
C
      CALL LEQT1C(Q,NELE,NELE,B,1,NELE,0,WA,IER)
C
      WRITE(*,130)(B(I),I=1,NELE)
130   FORMAT(1X,11HWEIGHTS ARE,(E15.9,5X,E15.9))
C
C        COMPUTE THE ANTENNA PATTERN
C     GENERATED BY THE COMPUTED WEIGHTS
C
      DO 220 I=1,361
      THETA = 2.0*PI*FREQ*SIN(FLOAT(I-1)*PI/180.0)
      DO 210 J=1,NELE
      X=CMPLX(COS(FLOAT(J)*THETA),SIN(FLOAT(J)*THETA))
      G(I) = G(I) + B(J)*X
210   CONTINUE
220   CONTINUE
C
      DO 240 I=1,361
      WRITE(*,230) I-1,G(I)
230   FORMAT(1X,2HAT,I3,7HDEGREES,3X,E15.9,5X,E15.9)
240   CONTINUE
      RETURN
      END
```

Vita

Linden Beattie Mercer was born on 15 May 1959 in Enid, Oklahoma. He graduated from Enid High School in 1977 and attended Oklahoma State University where he received the degree of Bachelor of Science in Electrical Engineering. After graduation, he entered the electro-optics program in the School of Engineering at the Air Force Institute of Technology in June 1981. He is registered as an Engineer-in-Training in the state of Oklahoma and is a member of Eta Kappa Nu, Tau Beta Pi, and Phi Kappa Phi.

Unclassified

SECURITY CLASSIFICATION OF THIS PAGE *(When Data Entered)*

REPORT DOCUMENTATION PAGE		READ INSTRUCTIONS BEFORE COMPLETING FORM
1. REPORT NUMBER AFIT/GEO/EE/82D-5	2. GOVT ACCESSION NO. AD-A124672	3. RECIPIENT'S CATALOG NUMBER
4. TITLE *(and Subtitle)* A TIME INTEGRATING OPTICAL OCRRELATOR FOR ADAPTIVE ARRAY PROCESSING		5. TYPE OF REPORT & PERIOD COVERED MS Thesis 6. PERFORMING ORG. REPORT NUMBER
7. AUTHOR(s) Linden B. Mercer Lieutenant USAF		8. CONTRACT OR GRANT NUMBER(s)
9. PERFORMING ORGANIZATION NAME AND ADDRESS Air Force Institute of Technology (AFIT/EN) Wright-Patterson AFB, OH 45433		10. PROGRAM ELEMENT, PROJECT, TASK AREA & WORK UNIT NUMBERS
11. CONTROLLING OFFICE NAME AND ADDRESS FDT/TQ, Wright-Patterson AFB, OH 45433		12. REPORT DATE December 1982 13. NUMBER OF PAGES
14. MONITORING AGENCY NAME & ADDRESS*(if different from Controlling Office)*		15. SECURITY CLASS. *(of this report)* UNCLASSIFIED 15a. DECLASSIFICATION/DOWNGRADING SCHEDULE

16. DISTRIBUTION STATEMENT *(of this Report)*

Approved for public release; distribution unlimited

17. DISTRIBUTION STATEMENT *(of the abstract entered in Block 20, if different from Report)*

18. SUPPLEMENTARY NOTES

Approved for public release: IAW AFR 190-17.

LYNN E. WOLAVER
Dean for Research and Professional Development
Air Force Institute of Technology (ATC)
Wright-Patterson AFB OH 45433

4 JAN 1983

19. KEY WORDS *(Continue on reverse side if necessary and identify by block number)*

Adaptive Arrays
Optical Signal Processing
Time Integrating Optical Correlators

20. ABSTRACT *(Continue on reverse side if necessary and identify by block number)*

Application of optical signal processing techniques to adaptive array processing was investigated. The common adaptive array algorithms were reviewed. Adaptive array processing generally requires some form of correlation and the characteristics of optical correlators were compared leading to the selection of the time integrating optical correlator for further investigation. An adaptive array processor using time integrating optical correlators, which was first proposed by David Casasent, was analyzed to determine applicability of this signal processing technique to a general

DD FORM 1 JAN 73 1473 EDITION OF 1 NOV 65 IS OBSOLETE

Unclassified

adaptive array environment. This processor was found to be similar to a comparable maximum likelihood approach. Limitations on the performance of this processor in terms of ambiguity and resolution were found and these results were confirmed by computer simulation of the adaptive array environment, the processor, and the resulting antenna response.

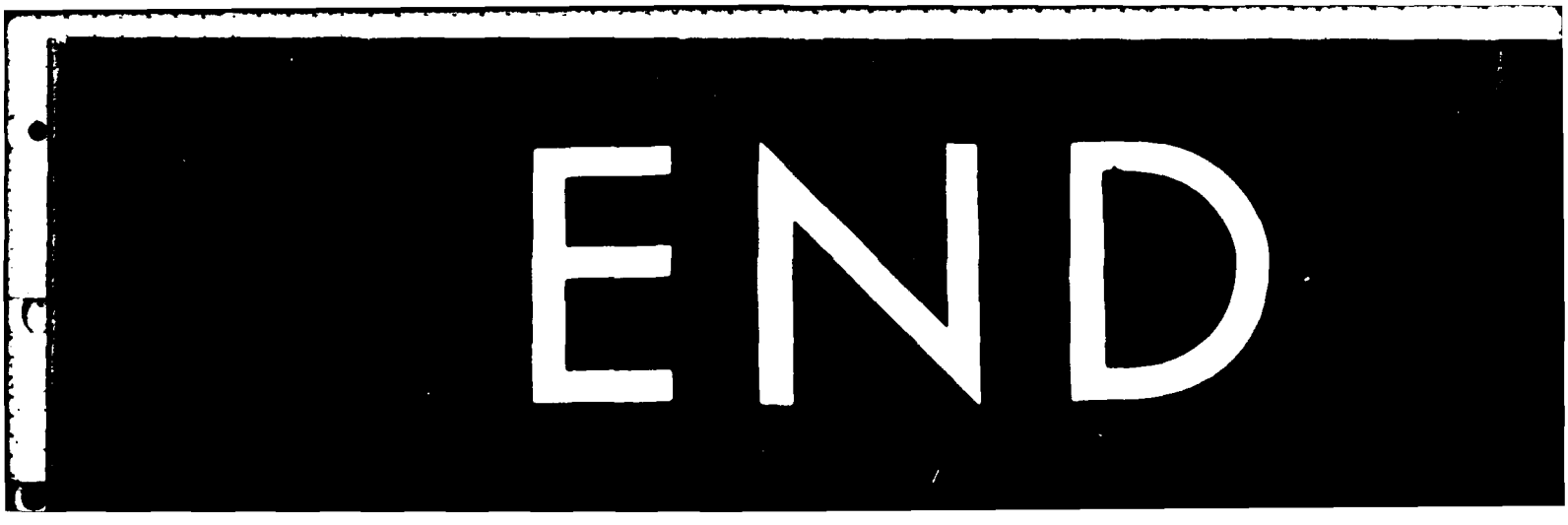
END